An integrative approach to identify and experimentally validate environmental variables which affect SCTLD outcomes













An integrative approach to identify and experimentally validate environmental variables which affect SCTLD outcomes

Prepared By:

Nicholas P. Jones¹, Sydney Dutton², Erin Shilling², Lauren Fuess²

¹National Coral Reef Institute, Halmos College of Arts and Sciences, Nova Southeastern University, 8000 N Ocean Drive, Dania Beach, Florida, 33004, USA

²Texas State University, San Marcos, Texas

June 2025

Completed in Fulfillment of [PO C40115] for
Florida Department of Environmental Protection
Coral Protection and Restoration Program
8000 N Ocean Dr.
Dania Beach, FL 33004

This report should be cited as follows:

Jones NP, Dutton S, Shilling S, Fuess L (2025) An integrative approach to identify and experimentally validate environmental variables which affect SCTLD outcomes. Award no. C40115. Florida Department of Environmental Protection. Miami, Fl, 1-38

This report was funded through a contract agreement from the Florida Department of Environmental Protection's (DEP) Coral Protection and Restoration Program. The views, statements, findings, conclusions, and recommendations expressed herein are those of the author(s) and do not necessarily reflect the views of the State of Florida or any of its subagencies.



Acknowledgements

We would like to thank all CREMP, SECREMP and DRM researchers who collected field data, NASA and NOAA for satellite data and the Southeast Florida Reef Tract Water Quality Assessment Project and the Southeast Environmental Research Center for collecting in situ water quality data. Special thanks to the Coral Reef Restoration Assessment and Monitoring lab at Nova Southeastern University for supplying coral colonies. We would also like to thank the Florida Department of Environmental Protection Florida's Coral Reef Resilience Program Grant for funding this project.

Management Summary

Disease outbreaks have caused mass coral mortality on Florida's Coral Reef (FCR) and continue to threaten the persistence of coral populations. Spatiotemporal variations in disease dynamics suggest environmental conditions influence disease susceptibility. Understanding these may allow us to identify the environmental factors which underpin coral health and predict future disease dynamics. We took an integrative approach, combining field observations and statistical modelling to identify the environmental drivers of disease susceptibility and severity on FCR, and performed lab experiments under these conditions to understand their effect on immunity in Montastraea cavernosa. Disease susceptibility was most strongly influenced by the interactions between maximum temperature and maximum chlorophyll-a concentration the month prior to the disease survey, and between maximum chlorophyll-a concentration and three month mean PAR. Disease probability was highest when chlorophyll-a concentration (nutrients proxy) exceeded ~6 mg m⁻³ and maximum temperatures were low (<30 °C) or when PAR and chlorophyll-a concentrations were high. Disease severity had a significant negative relationship with maximum temperature, where a colony had a 50% chance of dying unless temperatures exceeded 31.08 °C. Lab experimentation was conducted under conditions experienced on FCR to investigate the influence of temperature and nutrients on immune response. After one month of environmental manipulation, coral fragments were immune challenged to assess immune response. Heat stress largely drove broad suppression of constitutive immunity (peroxidase, phenoloxidase, and antibacterial activity), but increased catalase activity, which suggests stress within the host. These results suggest further disease outbreaks are likely as ocean temperatures increase. Corals exposed to moderate levels of ammonia (0.01 mg/1) induced the strongest immune responses (catalase and phenoloxidase activity), but that ceased under high concentrations (0.05 mg/l). Experimental nutrient enrichment conditions are experienced on FCR, and results suggest reducing ammonia in these locations could improve coral immunity and reduce the likelihood of another disease outbreak.

1

Executive Summary

Disease outbreaks have caused mass coral mortality on Florida's Coral Reef (FCR) and continue to threaten the persistence of coral populations. Spatiotemporal variations in disease dynamics suggest environmental conditions influence susceptibility, the probability of contracting disease, and severity, the probability of dying from disease. Understanding these variations may allow us to identify the factors which underpin coral health and predict future disease dynamics. We combined field observations and statistical modelling to identify the environmental conditions that influenced disease dynamics during the SCTLD outbreak, and performed lab experiments under these conditions to understand their effect on immunity in *Montastraea cavernosa*.

Disease susceptibility was quantified using data collected during the peak SCTLD outbreak. Disease severity was calculated as the change in *M. cavernosa* abundance at CREMP and SECREMP sites in the first two years following the outbreak. Environmental predictors were quantified using in situ and satellite data. Disease susceptibility and severity were modelled against these predictors in a two-step process using random forests and generalized linear mixed models.

Disease susceptibility was most strongly influenced by the interactions between maximum temperature and maximum chlorophyll-a concentration (nutrient proxy) the month prior to the disease survey, and between maximum chlorophyll-a and three-month mean PAR prior to the disease survey. Disease probability was highest when chlorophyll-a concentration exceeded ~6 mg m⁻³ and maximum temperatures were below 30 °C or when mean PAR and chlorophyll-a concentrations were high. Disease severity had a negative relationship with maximum temperature, such that unless temperatures exceeded 31.08 °C there was an over 50% chance of a colony dying.

Lab experimentation investigated the impact of temperature and nutrients, the interaction identified as most strongly influencing disease susceptibility, on coral immune response. A crossed design with six treatments reflective of conditions experienced on FCR was used: temperature (high or ambient) and nutrients (none, moderate or high). After one month of environmental manipulation, coral fragments were immune challenged by pathogenic stimuli or placebo to assess immune response. Multivariate analysis revealed strong impacts of temperature, nutrients (ammonia concentration), and the interaction of nutrients and immune challenge. Heat stress largely drove broad suppression of constitutive immunity (peroxidase, phenoloxidase, and antibacterial activity), but increased catalase activity. Corals exposed to moderate levels of ammonia (0.01 mg/1) induced the strongest immune responses (catalase and phenoloxidase activity), but this benefit was lost at high concentrations (0.05 mg/l).

Our results suggest temperature played the primary role in SCTLD susceptibility and severity and that it strongly influences immune response. Temperatures which likely induced bleaching were related to reduced SCTLD severity, strengthening findings that suggest it initially affected Symbiodiniaceae before causing host tissue loss. However, lab experiments found multiple immune metrics were suppressed at elevated temperatures, while enhanced catalase activity suggests stress within the coral, suggesting further disease outbreaks are likely as ocean temperatures rise. Both methods suggest that under eutrophic conditions immune response is lower and disease susceptibility increases. The experimental eutrophic conditions are experienced on FCR, and our results suggest reducing ammonia in these locations could improve coral immunity and reduce the likelihood of another major disease outbreak.

2 C40115

Table of Contents

1. Introd	duction	4
2. Goal	1: Identify environmental drivers of disease	5
2.1.	Methods	5
2.1.1.	Coral disease data	5
2.1.2.	Environmental predictors	6
2.2.	Results	9
2.2.1.	Disease susceptibility	9
2.2.2.	Disease severity	11
3. Goal	2: Experimentally validate effect of environmental conditions on disease	13
3.1.	Methods	13
3.1.1.	Coral Collection and Husbandry	13
3.1.2.	Experimental Approach- Environmental Manipulations	14
3.1.3	Experimental Approach- Immune Challenges	16
3.1.4	Sample Processing	16
3.1.5.	Statistical Analysis	17
3.2.	Results	18
3.2.1.	Multivariate Analyses	18
3.2.2.	Univariate Analyses	24
4. Goal	3: Model disease probability and identify resistant locations	29
4.1.	Methods	29
4.2.	Results	29
5. Discu	ssion and management recommendations	34
6 Refer	rences	36

1. Introduction

Disease outbreaks, such as Stony Coral Tissue Loss Disease (SCTLD), have caused mass stony coral mortality on Florida's Coral Reef (FCR) in recent decades and continue to threaten the persistence of coral populations. While the broadscale impacts of SCTLD have been severe, spatiotemporal differences in disease susceptibility and severity in FCR and the wider Caribbean (e.g., Alvarez-Filip et al. 2019; Rippe et al. 2019; Muller et al. 2020; Williams et al. 2021) suggest local environmental conditions exacerbated SCTLD susceptibility and enhanced coral mortality. To date, no clear environmental pattern has been identified to explain the spatiotemporal variations in SCTLD etiology or epidemiology. Initial outbreak reports suggested an environmental trigger, primarily prolonged heat stress (Precht et al. 2016; Jones et al. 2021), and while there are suggestions that the subsequent spread and peaks in SCTLD elsewhere in Florida were not associated with heating (Muller et al. 2020; Williams et al. 2021), elsewhere in the Caribbean poor water quality has been implicated as exacerbating coral mortality (Alvarez-Filip et al. 2019; Alvarez-Filip et al. 2022). Regardless of the exact trigger, it remains plausible that environmental conditions predisposed coral communities in Florida to disease, as has been found in other diseases and in other locations (Voss & Richardson 2006; Lesser et al. 2007; Muller & van Woesik 2009; Ban et al. 2014; van Woesik & Randall 2017; Muller et al. 2018; Lapointe et al. 2019; Donovan et al. 2021) and that they will continue to increase disease susceptibility and reduce coral recovery potential (Jones & Gilliam 2024).

Spatiotemporal differences in multi-species disease outbreaks can be compounded by variability in community composition and interspecific variation in susceptibility. This makes it difficult to disentangle the environmental drivers of disease from spatial variations in diversity. Hence, studying disease dynamics in a single, widely distributed species increases confidence that spatiotemporal patterns are related to environmental conditions, and not stony coral community composition (i.e., the proportion of highly susceptible species). *Montastraea cavernosa* is a moderately SCTLD susceptible, massive species which is found widely across FCR. Previous studies assessing the effect of SCTLD on *M. cavernosa* found temporal (Shilling et al. 2021) and spatial (Aeby et al. 2019) variability in lesion development and lesion progression rates, both of which raise the potential of environmental influence on both disease susceptibility (i.e., the probability of a colony becoming diseased) and disease severity (i.e., the probability of colony mortality once infected).

Identifying the specific environmental conditions which influenced disease susceptibility and severity during the SCTLD outbreak may also allow us to identify the environmental factors which underpin coral health and predict future disease dynamics. A number of environmental conditions, including thermal stress (e.g., Bruno et al. 2007; Miller et al. 2009), nutrient enrichment (e.g., Vega Thurber et al 2014) and suspended sediments/turbidity (e.g., Pollock et al. 2014) have been associated with inducing and exacerbating disease outbreaks. These relationships have generally been identified through field data, which identify correlations, but not causation, or laboratory experiments, which may not be ecologically relevant. By integrating both approaches, it may be possible to identify ecologically meaningful environmental variables and experimentally validate that they influence disease. Furthermore, by taking a laboratory approach grounded in

understanding the effects of identified environmental covariates on coral immunity and pathogen susceptibility generally (as opposed to purely a specific disease such as SCTLD), the results provide generalizable insight regarding the impacts of environmental conditions on general coral disease susceptibility. The results of the combined approach can be used to create predictive models which have the ability to identify locations more susceptible to future disease outbreaks and to inform management actions.

In this study, we used the SCTLD outbreak as a case study and took an integrative approach to identify environmental conditions that influence disease susceptibility and severity in *M. cavernosa*. We combined field observations, statistical modelling and lab experimentation to answer three research questions: 1) Did environmental conditions exacerbate SCTLD susceptibility and severity in *M. cavernosa*? 2) If so, do these environmental variables actually influence *M. cavernosa* immunity and general pathogen susceptibility? Then, using the identified environmental conditions which influenced disease susceptibility, 3) Where are locations predicted to be more or less susceptible to future disease outbreaks?

2. Goal 1: Identify environmental drivers of disease

2.1. Methods

2.1.1. Coral disease data

Disease susceptibility was quantified as disease prevalence (i.e., the proportion of *M. cavernosa* colonies with SCTLD) at individual sites surveyed as part of the Coral Reef Evaluation and Monitoring Project (CREMP), Southeast Florida Coral Reef Evaluation and Monitoring Project (SECREMP) and the Florida Reef Resilience Program's (FRRP) Disturbance Response Monitoring (DRM). If sites had multiple transects, *M. cavernosa* abundance and disease prevalence were summed to the site level. As the spread of SCTLD varied spatiotemporally across FCR, disease prevalence data was filtered to capture the peak disease outbreak period in each FCR subregion using previously documented timelines (e.g., Walton et al. 2018; Muller et al. 2020; Williams et al. 2021; Hayes et al. 2022) and by visually assessing spatiotemporal variation in disease prevalence. The peak disease outbreak period was considered to be from 2014-2016 throughout the Kristin Jacobs Coral Aquatic Preserve (Coral AP): Martin, Palm Beach, Deerfield, Broward, Miami and Biscayne; from 2016 to 2018 in the Upper and Middle Keys, from 2018 to 2019 in the Lower Keys and Marquesas; from 2019 to 2022 in the Marquesas-Tortugas transition zone and from 2020 to 2022 in the Dry Tortugas.

Disease severity was quantified as the mortality rate (i.e., the relative change in M. cavernosa abundance) during the initial two years of the SCTLD outbreak at CREMP and SECREMP sites. Abundance at CREMP sites was counted on four, $10 \text{ m} \times 1 \text{ m}$ transects, and at SECREMP sites on four, $22 \text{ m} \times 1 \text{ m}$ transects. At each site, abundance was summed per site per year. The mortality rate was calculated as the change in abundance from year 0 to year 2, divided by the initial abundance (i.e., relative change (% yr⁻¹)). Only colonies $\geq 4 \text{ cm}$ maximum diameter were counted to avoid capturing colonies that recruited during the disease outbreak. Two years was considered

sufficient time for colonies which became diseased during the peak outbreak period to have died and to avoid capturing recruits that grew into the adult dataset by the second year (e.g., Jones & Gilliam 2024). To capture the peak in mortality rate at each site, mortality rates were calculated for multiple two-year periods and the period chosen, that during which the largest relative change in M. cavernosa abundance occurred at each site. The period generally stayed consistent within a subregion such that the chosen period was 2014 to 2016 in Broward, Miami and Biscayne, 2015 to 2017 in Martin, Palm Beach and Deerfield, 2016 to 2018 in the Upper and Middle Keys, 2017 to 2019 in the Lower Keys and 2020 to 2022 in the Dry Tortugas.

2.1.2. Environmental predictors

Environmental data prior to the peak disease outbreak and during the outbreak period were compiled from in situ and satellite data, and specific environmental predictors calculated for their relevance to stress responses in stony corals at each benthic sampling site. Data from NASA's Moderate Resolution Imaging Spectroradiometer satellite (MODIS Aqua) was used to measure solar irradiance, diffuse attenuation coefficient (turbidity proxy) and chlorophyll-a concentration (nutrients proxy). Irradiance was obtained as the surface downwelling photosynthetic flux in air (Photosynthetically Available Radiation (PAR) einstein m⁻² s⁻¹) and diffuse attenuation coefficient kD490 $(m^{-1}).$ Data were extracted from NASA's Ocean color (https://oceancolor.gsfc.nasa.gov/13/) as the monthly mean for each metric at 1/25th resolution throughout Florida. Data was visually assessed and any obvious outliers removed. Temperature data was obtained from satellite and in situ sampling. Degree heating week data was obtained from NOAA's Coral Reef Watch (NOAA CRW 2018). Daily in situ temperature data was collected by HOBO v2 temperature loggers at CREMP and SECREMP sites throughout FCR.

The environmental regime at each benthic sampling site was calculated using a spatial join with the in situ and satellite data. Each benthic site was joined with the three closest satellite sites and the monthly mean of each variable calculated per benthic site. To calculate the temperature regime at DRM sites which were used in the disease susceptibility analysis, a spatial join was made to the nearest CREMP/SECREMP site. If the closest CREMP/SECREMP site had missing data then a spatial join was made to the closest two sites. After the database with the environmental regime at each benthic site was created, multiple environmental predictors were created to represent conditions either leading up to the disease susceptibility surveys or in the time between disease severity surveys.

For the disease susceptibility analysis, each environmental variable: chlorophyll-a concentration, PAR, kD490 and temperature, the maximum and mean values were quantified within the month prior, within the prior three months and within the prior year to the benthic survey. To further capture the temperature regime at a site, the minimum temperature one month, three months and one year prior to the benthic survey and specific thermal stress predictors were calculated. Thermal thresholds were calculated independently for each subregion using modelled SST data from the Hybrid Coordinate Ocean Model (HYCOM) from 2014 to 2022, as 1 °C above the maximum of the mean summertime (July-September) SST, or 1 °C below the minimum of the mean wintertime (January-March) SST as per Jones et al. (2020). The heat stress or cold stress durations were calculated for each site as the number of days in situ water temperature exceeded thermal

C40115

thresholds in the month, three months and year before a benthic survey. This gave 31 environmental predictors, which were tested for collinearity by calculating the Spearman's rank correlation coefficient, which is well suited to assess non-linear relationships and data which are non-normal. Correlations were considered significant at a threshold of 0.8 and one of the collinear predictors removed prior to statistical analysis. An attempt was made to keep at least one predictor of a variable at each time point. All chlorophyll-a and kD490 predictors were highly collinear and all removed except maximum chlorophyll-a the month prior to the survey as this was hypothesized to have the greatest effect on disease susceptibility. The removal of other collinear predictors left 15 environmental predictors which were used in statistical analysis (Table 1).

Table 1. Environmental summary of predictors used in disease susceptibility full random forest model. Variable = type of environmental variable, predictor = metric of that variable, time period = temporal duration predictor calculated over. e.g., chlorophyll-a maximum, is the maximum chlorophyll-a concentration within one month prior to the disease survey.

Variable	Predictor	Time period	Mean	SD
Chlorophyll-a (mg m ⁻³)	Maximum	One month	3.82	5.12
PAR (Einstein m ⁻² day ⁻¹)	Maximum	One month	48.16	6.11
PAR (Einstein m ⁻² day ⁻¹)	Maximum	Three months	56.68	2.50
PAR (Einstein m ⁻² day ⁻¹)	Maximum	One year	58.23	1.93
PAR (Einstein m ⁻² day ⁻¹)	Mean	Three months	51.74	3.16
PAR (Einstein m ⁻² day ⁻¹)	Mean	One year	43.42	1.52
Temperature (°C)	Maximum	One month	30.75	1.01
Temperature (°C)	Maximum	One year	31.36	0.61
Temperature (°C)	Mean	Three months	29.44	1.30
Temperature (°C)	Mean	One year	27.13	0.61
Temperature (°C)	Minimum	One year	21.51	1.70
Thermal stress	Heat stress	One month	0.93	2.77
Thermal stress	Heat stress	Three months	2.44	5.89
Thermal stress	Cold stress	One year	1.99	5.43
Thermal stress	DHW	At survey	1.34	1.81

For the disease severity analysis, the same environmental variables were used, but environmental predictors (e.g., maximum or mean temperature) were calculated over the year leading up to the initial benthic survey and in the two years between survey events. This gave 23 environmental predictors, which were tested for collinearity and removed in the same way as described above. The removal of collinear predictors gave 14 environmental predictors which were used in statistical analysis (Table 2).

7

Table 2. Environmental summary of predictors used in disease severity full random forest model. Variable = type of environmental variable, predictor = metric of that variable, time period = temporal duration predictor calculated over. e.g., Chlorophyll-a maximum year prior, is the maximum Chlorophyll-a concentration within the year prior to the initial benthic survey used to count *Montastraea cavernosa* abundance. PAR maximum during, is the maximum PAR measurement in the two years between monitoring surveys.

Variable	Predictor	Time period	Mean	SD
Chlorophyll-a (mg m ⁻³)	Maximum	Year prior	8.88	10.95
PAR (Einstein m ⁻² day ⁻¹)	Maximum	During	59.09	1.32
PAR (Einstein m ⁻² day ⁻¹)	Mean	During	43.52	1.55
Temperature (°C)	Maximum	Year prior	31.07	0.9
Temperature (°C)	Maximum	During	31.37	0.71
Temperature (°C)	Mean	Year prior	26.97	0.94
Temperature (°C)	Mean	During	27.07	0.35
Temperature (°C)	Minimum	Year prior	21.89	1.93
Temperature (°C)	Minimum	During	21.24	1.3
Thermal stress	Heat stress	Year prior	4.03	7.41
Thermal stress	Heat stress	During	6.68	11.89
Thermal stress	Cold stress	Year prior	2.21	6.15
Thermal stress	Cold stress	During	4.39	10.36
Thermal stress	Maximum DHW	During	1.73	2.15

2.1.3. Statistical analysis

To assess the relationship between disease susceptibility and disease severity with environmental predictors, univariate modelling was conducted in a two-step process in R (R Core Team, 2024). First, for each response metric, a random forest regression model was used to identify the most important predictors in variation in each response variable. The predictors which accounted for 75% of the variation in the full random forest model were retained and a backwards stepwise regression performed to identify the most important environmental predictors for stage two using the R². Partial regression plots were inspected for any evidence of quadratic relationships. The selected predictors were then modelled as either a binomial Generalized Linear Model (GLM), or binomial Generalized Linear Mixed Model (GLMM), which incorporated any potentially meaningful interactions between predictors.

Disease susceptibility (n = 939) was modelled as disease prevalence (i.e., the proportion of diseased M. cavernosa colonies at the time of sampling) in both the random forest and GLMM. In the GLMM, the abundance of M. cavernosa at a site was fitted as weights. Sub-region nested within year was fitted as a random effect to account for spatiotemporal variation in disease spread, as sites close together were predicted to be more likely to encounter SCTLD at the same time. Disease severity (n = 62) was modelled as mortality rate (i.e., the proportion of M. cavernosa colonies which died over the two-year peak outbreak period). In the random forest regression

model, the response variable was fitted as the relative change in abundance (% yr⁻¹). In the GLM, the response variable was fitted as the proportion that died (i.e., change /initial abundance), with the weights as the initial *M. cavernosa* abundance at the site. Model selection was conducted using a backwards stepwise approach from the full model, containing all predictors and meaningful interactions, by inspecting model summaries and comparing the Akaike Information Criteria (AIC).

Random forest model reliability and goodness of fit were visually assessed by plotting the cross-validation error rate against the number of trees, the root mean squared error (calculated using the out of bag samples) against fitted predictions and fitted model predictions against the observed data. The minimum adequate GLM was validated by plotting deviance residuals against fitted values, and deviance residuals against each significant variable in the fitted model. The fitted GLMM was validated using the package DHARMa with residual diagnostics, including overdispersion and heterogeneity, conducted on the fitted model (Hartig 2017). Overdispersion was detected in the disease severity GLM, the model refit with a quasibinomial distribution and model selection repeated as above. Two outliers were detected and removed. Model validation indicated no further problems. The variance inflation factor (VIF) was used to check fitted models for multicollinearity.

2.2. Results

2.2.1. Disease susceptibility

Disease prevalence was most strongly influenced by the interactions between maximum temperature and maximum chlorophyll-a concentration the month prior to the disease survey, and between maximum chlorophyll-a concentration and three-month mean PAR prior to the disease survey. Disease probability increased with maximum temperature until maximum chlorophyll concentration exceeded ~2 mg m⁻³, with colonies 50-60% more likely to be diseased with each unit increase in temperature (Figure 1a). Around the mean regional maximum chlorophyll-a concentration (3.8 mg m⁻³), there was a slight negative relationship between maximum temperature and disease prevalence, but this was not significantly different to zero until chlorophyll-a concentration exceeded ~6 mg m⁻³. Then the probability of a colony being diseased declined substantially with maximum temperature. Disease probability declined with maximum chlorophyll-a concentration when the three-month mean PAR was below or equal to the FCR mean (52 einsteins m⁻² s⁻¹), but increased with chlorophyll-a concentration if three-month mean PAR was greater than the FCR mean (Figure 1b).

9

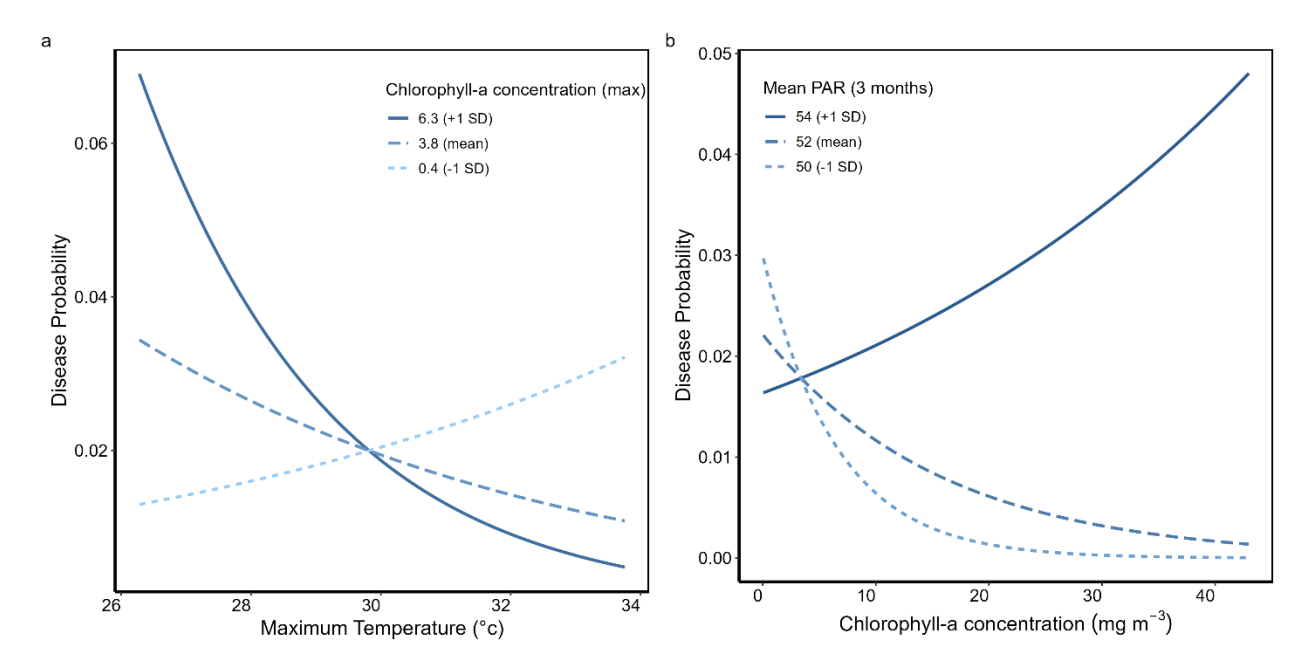


Figure 1. The greatest amount of variation in disease susceptibility was explained by the interaction between a) maximum temperature and maximum chlorophyll-a concentration, then b) maximum chlorophyll-a concentration and three-month mean PAR. When the maximum chlorophyll-a concentration one month before the survey was below the regional mean, colonies were 50-60% more likely to be diseased with each unit increase in maximum temperature. Colonies were ~two times less likely to be diseased with each unit increase in maximum temperature when the maximum chlorophyll-a concentration was 6 mg m⁻³. When mean PAR was below or equal to the regional mean, colonies were ~two times less likely to be diseased with each unit increase in chlorophyll-a, but ~50% more likely to be diseased with each unit increase in chlorophyll-a when mean PAR was above the regional mean.

The probability of a colony being diseased also significantly increased with maximum PAR and declined with the mean temperature three months before surveying (GLMM; conditional $R^2 = 0.7$, Marginal $R^2 = 0.1$; Table 3). Colonies were 50% more likely to be diseased with every unit increase in maximum PAR and two times less likely to be diseased with every unit increase in three-month mean temperature. As indicated by the high conditional R^2 , survey location/time had a very large effect on disease prevalence.

Table 3. Significant predictors of disease prevalence (Note: maximum chlorophyll-a concentration retained due to presence in interactions) from GLMM. Estimate gives effect size on the logit scale. Negative estimate indicates a negative relationship between predictor and disease prevalence.

10

Environmental predictor	Estimate	Std. Error	z value	p value
(Intercept)	-0.57	4.13	-0.14	0.9
Max temperature	0.44	0.18	2.40	0.02
Max PAR	0.05	0.02	2.64	0.008
3-month mean temperature	-0.29	0.14	-2.03	0.04

Max Chl-a	0.49	0.54	0.91	0.4
3-month mean PAR	-0.22	0.05	-4.48	0.000007
Max temp x Max Chl-a	-0.09	0.02	-3.95	0.00008
Max Chl-a x 3 month mean PAR	0.04	0.01	4.58	0.000005

2.2.2. Disease severity

The probability of a colony dying significantly declined with maximum temperature during the disease outbreak (GLM; $R^2 = 0.56$), such that for every unit increase in maximum temperature, which averaged 31.4 °C (\pm 0.7 SD), colony mortality was three times less likely (Figure 2). Below 31.08 °C the fitted GLM predicted there was a greater than 50% chance that an *M. cavernosa* colony would die. No other environmental predictor significantly affected mortality probability (Table 4).

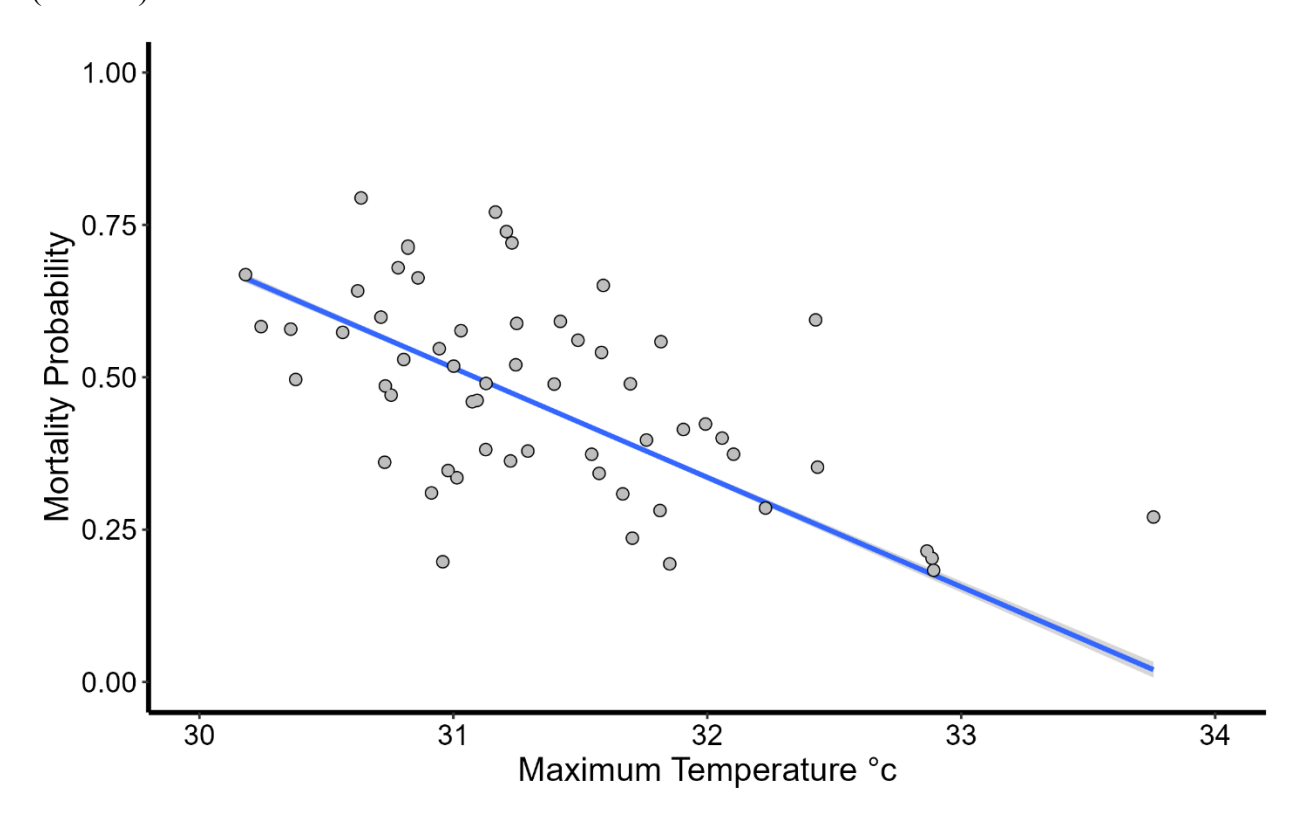


Figure 2. Modelled relationship between mortality probability (i.e., disease severity) and the maximum temperature in the two years between surveys. $R^2 = 0.56$. Blue line = mean mortality probability; grey points = model estimates for individual survey sites.

Table 4. GLM summary of relationship between disease severity (modelled as mortality probability) and the most important environmental predictors. Only the maximum temperature between survey periods significantly influenced mortality probability.

Environmental	Estimate	Std. Error	t value	p value
predictor				
(Intercept)	25.40	3.15	8.08	5.1 e-11
Max temperature	-0.82	0.10	-8.15	3.9 e-11

3. Goal 2: Experimentally validate effect of environmental conditions on disease

3.1. Methods

3.1.1. Coral Collection and Husbandry

Fragments of nine unique genets of *Montastraea cavernosa* were collected from the NSU Coral Reef Restoration, Assessment and Monitoring labs offshore coral nursery and shipped to Texas State University in early February 2025. Due to shipping delays, corals arrived in various health states and were immediately screened upon arrival for abrasions, lesions, necrosis, and mortality. Fragments with mortality greater than 90% were removed from experimental groups. The remaining fragments were then tagged based on genotype and placed in recirculating tanks for long term husbandry and experimentation. The Fuess Lab aquaria system consists of connected (but able to be isolated) ten-gallon tanks which have recirculating artificial sea water (ASW), automated lighting, heating, and buffer solution dosing. The system includes multiple biological and mechanical filtration steps and UV sterilization for circulating water. Prior to experimentation, corals were maintained in this system at conditions recommended by coral aquarists at Nova Southeastern University which were based on local reef conditions: 35 ppt salinity, 24°C, 7.2 dKH, 400 ppm Ca, 1400 ppm Mg, and 0 ppm NH4, NO3, and NO2. Light levels were kept at approximately 50 μM/m2s for 11.5 hours daily with a 30-minute ramp up/down period each morning and evening to mimic the current sunrise and sunset in Fort Lauderdale, FL.

Corals were maintained at stable conditions for an acclimatization period of two and a half weeks, with additional steps to facilitate recovery from shipping stress. Specifically, for the first week of this period, corals were dosed with RESTOR and tanks underwent 50-75% water changes daily. This treatment was necessary while corals were recovering from shipping stress. Once corals had stabilized (after one week at TXST), corals transitioned to standard care consisting of twice weekly feeding with hatched Artemia shrimp followed by 20% water changes. This feeding and water change schedule was maintained through the duration of the experiment. Two weeks after arrival, corals were slowly acclimatized to average summer temperatures on FCR. This involved a gradual temperature increase from temperature at collection, ~24 °C, to a final temperature of 28°C. Temperatures were raised 1 degree every two days to achieve this acclimatization. A control temperature of 28°C was chosen based on modeling results (Figure 1). A clear shift in the relationship between chlorophyll concentration (proxy for nutrient enrichment) and disease susceptibility was observed at 30°C. Therefore, we chose control (28°C) and heat stress (32°C) temperatures equidistant from that shift point for our experiment so as to capture this shifting relationship.

Two and a half weeks after arrival, corals were fragged using a Gryphon Diamond Band Saw. All received frags were cut up into approximately 3 x 3 cm smaller frags and tagged. Enough coral frags survived and were able to be split into enough replicates to use seven genotypes for the experiment. These frags were then allowed to recover from fragging for another two weeks before starting the experiment. A full schedule of major coral husbandry events from colony arrival to the end of the experiment is shown in Table 5.

Table 5. Full schedule of coral husbandry events from arrival through the curation of the experiment.

Date	Event
Feb 7 th	Corals arrived
Feb 7 th	RESTOR dosing began
Feb 8 th	50% - 75% water changes began
Feb 14 th	50% - 75% water changes end
Feb 14 th	RESTOR dosing end
Feb 21st	Temperature ramping to 28 °C began
Feb 25 th	Corals fragged
Feb 26 th	Corals fragged
Mar 7 th	Temperature ramping to 28 °C end
March 14th	Experiment start
March 14th	Heat tank temperature ramping to 32 °C
	began
March 17 th	Heat tank temperature ramping to 32 °C
	end
April 15 th	Corals injected
April 16 th	Experiment end

3.1.2. Experimental Approach- Environmental Manipulations

After a total acclimatization period of roughly one-month, experimentation was conducted to investigate the impact of temperature and nutrients, the interaction identified as most strongly influencing disease susceptibility and the single factor, temperature, which influenced disease severity during modelling, on coral immune response. Coral pieces were randomly assigned to one of six treatments representing a full factorial combination of the two factors: temperature (ambient or heat) and nutrient enrichment (none, mid, high; Table 6). Pieces were then split across six tanks representing each of the six treatments; pieces of genets were divided so that two pieces per genet were present in each treatment group. Tanks were isolated from the recirculating system for the duration of the experiment to prevent cross-contamination of temperature or ammonia treatment. Individual heaters were used to raise temperatures in the three heat stress tanks; temperature was ramped from 28 °C to 32 °C at a rate of 1 °C per day. Temperature in all tanks was monitored throughout the duration of the experiment via HOBO Onset Data Loggers. Figure 3 displays the experimental setup.

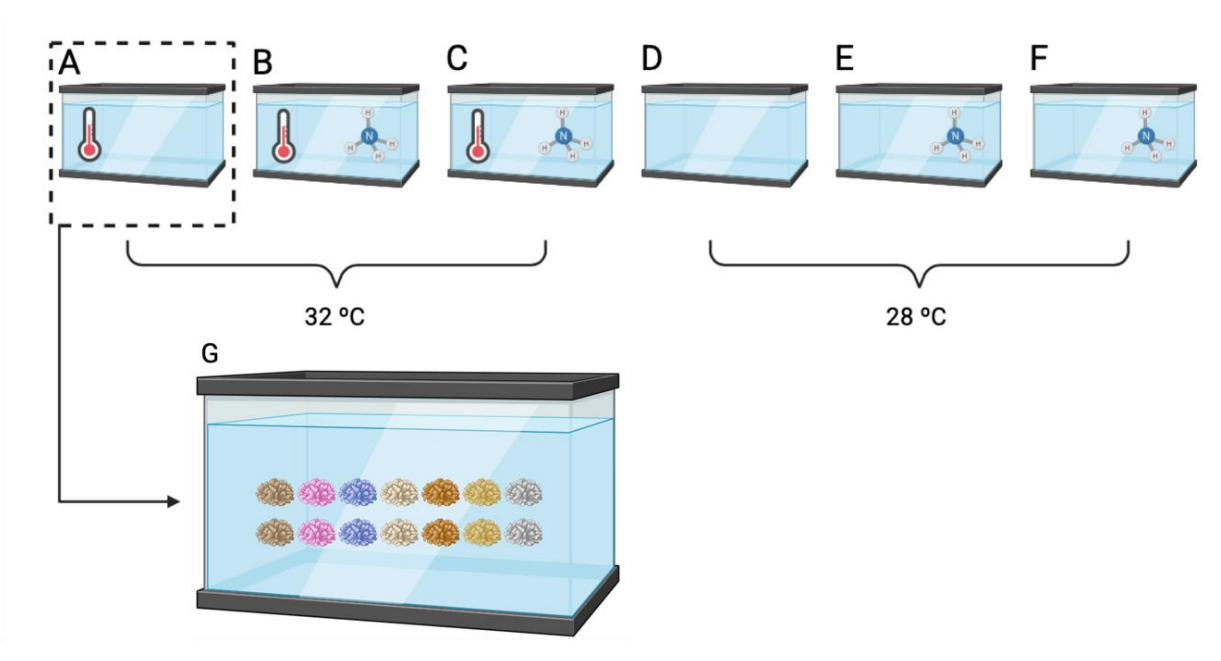


Figure 3. Experiment tank set up showing environmental manipulations. (A) heat only, (B) heat and mid nutrients (0.01 mg/L NH₄), (C) heat and high nutrients (0.05 mg/L NH₄), (D) full control, (E) ambient and mid nutrients (0.01 mg/L NH₄), (F) ambient and high nutrients (0.05 mg/L NH₄). (G) Example of tank showing the fourteen frags in each tank, 2 frags from each of the seven genotypes.

Nutrient enrichment was conducted via the addition of ammonia with concentrations selected to reflect environmental conditions on FCR (Jones and Gilliam 2024). Ammonia was chosen to represent chlorophyll-a as it is the preferred nutrient source for zooxanthellae (Morris et al. 2019), the density of which we predicted influenced SCTLD susceptibility. At the start of the experiment, nutrient amended tanks were dosed with ammonium chloride (NH₄Cl, CAS # 12125-02-9) to reach their respective dosage. After initial dosing, levels were measured twice a week in all six tanks using a modification of the phenate method (Solorzano 1969). The modification involved using sodium citrate (Na₃C₆H₅O₇, CAS # 6132-04-3), as a complexing agent to eliminate interference of calcium and magnesium (APHA 2023). After testing ammonia concentrations, tanks were dosed as needed to maintain the desired concentration. Additionally, when 30% water changes were conducted on feeding days, the ASW used to replace the water removed was dosed with NH₄Cl to match the target concentration for the respective tank (i.e. the mid-nutrient tank was given ASW at a concentration of 0.01 mg/L of NH₄). Temperature and nutrient enrichment treatments were maintained for one month before immune challenge experiments to mimic disease susceptibility modelling results (the interaction between maximum temperature and maximum chlorophyll concentration in the month before survey).

Table 6. List of environmental treatment types including final temperature and ammonia values. Each treatment type corresponds to a single experimental tank. Treatments listed were crossed with immune challenge treatment (placebo or immune challenge) in a full factorial manner for a final total of 12 treatment groups.

Treatment	Temperature	Ammonia
Ambient,	28 °C	0
None		
Ambient, Mid	28 °C	0.01 mg/L
Ambient, High	28 °C	0.05 mg/L
Heat, None	32 °C	0
Heat, Mid	32 °C	0.01 mg/L
Heat, None	32 °C	0.05 mg/L

3.1.3. Experimental Approach-Immune Challenges

Following one month of environmental manipulation, we conducted an experimental immune challenge to assess the impact of varied environmental conditions on response to pathogenic stimuli. Fragments within each treatment tank were randomly assigned to one of two treatments: placebo or immune stimuli. Assignments were made to ensure a full factorial combination of treatments (temperature x nutrient x immune challenge), with one fragment per genet in each of the 12 treatment groups. Each fragment was placed into an aerated, individual 500 mL, autoclaved plastic beaker with ~400 mL of 0.2 µm filtered ASW at 35 ppt. For ease of experimentation, ammonia treatment was not continued through the immune challenge portion of the experiment. Individual beakers were randomly placed into larger aquaria, which served as water baths maintaining a temperature of 28 °C or 32 °C (respective of their original treatment) within the beakers. Coral fragments were allowed to acclimate in the beakers for two hours and were then injected with 500 uL of one of two treatments: heat-killed bacteria, Vibrio coralliilyticus at 1 x 108 CFU/mL in sterile ASW, or sterile ASW (vehicle control). Injections were split across 5 locations in the fragment with ~100 uL injected in each location, for a total injection volume of 500 uL. Corals were then incubated for 12 hours before sampling for immune assays (i.e. flash freezing).

3.1.4. Sample Processing

To prepare fragments for immune assays, tissue was removed from frozen coral fragments using a Paasche airbrush and 100 mM Tris + 0.05mM DTT (pH 7.8) buffer. This tissue slurry was homogenized for 1 minute and placed on ice for 7 – 10 minutes. A 1 mL aliquot of tissue slurry was taken for melanin analysis, placed into a pre-weighed 1.5 mL tube and flash frozen, then stored at -20° C until analysis. The remaining tissue slurry was centrifuged at 3500 rpm for 5 min, after which two aliquots of the supernatant (aka protein extract) were transferred into 2 mL tubes and flash frozen, then stored at -80 °C until being used in all other protein analyses.

Immune assays were conducted in triplicate, including negative controls using the Tris+DTT buffer used to homogenize, and were measured on the BioTek Cytation 1 imaging reader, unless specified otherwise. Protein concentration was measured for each sample before conducting any assays using a Red660 assay. Protein extract (10 uL) was combined with 150 uL of G-Biosciences Red660. Sample absorbance was read at 660 nm and compared to a bovine serum albumin (BSA) standard curve to determine sample protein concentration. Measurements from subsequent assays were all standardized by protein concentrations unless otherwise indicated.

Antioxidant activity was measured using catalase and peroxidase activity assays following established methods (Changsut et al., 2022; Fuess et al., 2016). To measure catalase activity, 5 uL of protein extract is combined with 45 uL of 50 mM phosphate-buffered saline pH 7.0 (PBS) and 75 uL of 25 mM H₂O₂. Negative controls of Tris+DTT and a set of serial dilution wells using the PBS and H₂O₂ are included as well. Changes in absorbance (catalase activity) are then measured every 45 seconds for 15 minutes at the 240 nm wavelength. Catalase activity is then calculated using the most linear part of the curve in the first 1-5 minutes of the reaction and standardized using the serial dilution curve. To measure peroxidase activity, 10 uL of protein extract is combined with 20 uL of 10 mM phosphate-buffered saline pH 6.0 (PBS), 25 uL of 5 mM of guaiacol, and 20 uL of 20 mM H₂O₂. Negative controls of Tris+DTT. Changes in absorbance (catalase activity) are then measured every 45 seconds for 15 minutes at the 470 nm wavelength. Peroxidase activity is then calculated using the entire curve.

Total Phenoloxidase Activity (TPO) was measured following existing protocols (Mydlarz & Palmer, 2011) by combining 20 uL of protein extract, 20 uL of 50 mM PBS pH 7.0, 25 uL of 0.1 mg/mL trypsin, and allowing this mixture to incubate at room temperature for 30 minutes. Then 30 uL of 10 mM dopamine was added, and changes in absorbance were immediately measured every 45 seconds for 15 min. at 490 nm. TPO activity was then calculated using the most linear part of the curve in the first 1-5 minutes of the reaction.

Antibacterial activity (AB) was quantified by measuring bacterial growth doubling time of V. coralliilyticus in the presence of host protein extracts (Changsut et al., 2022). Cultures of V. coralliilyticus were incubated with host protein extracts diluted to a standard protein concentration. Specifically, 60 μ L of sample (or buffer control) was added to 140 μ L of V. coralliilyticus diluted to an OD representative of the start of its bacterial growth curve (approximately 0.2). Absorbance at 600 nm was then read every 10 minutes for six hours to create a bacterial growth curve. Bacterial growth doubling time was calculated from the logarithmic growth phase.

3.1.5. Statistical Analysis

Generated immune metric data was analyzed to specifically assess the impacts of temperature and nutrient treatment (and the interaction thereof) on baseline immunity and immune response to stimuli. Prior to all analyses we used the R package mice to impute one missing catalase value using the pmm method with 5 imputed datasets and a maximum of 50 iterations. We began with multivariate analyses of the impacts of these three factors (temperature, nutrients, immune challenge) on all immunological data combined. Data was normalized and a PERMANOVA

analysis was run using the R package vegan with the adonis2 function using the model: immune metrics ~ Temperature * Nutrients * Immune Challenge (Martinez Arbizu, 2020; Oksanen et al., 2025). The random effect of genet was accounted for using the strata parameter, and we specified a Euclidean distance approach. Post-hoc pairwise comparisons were conducted for significant terms using a custom function with the same parameters as the main model and corrected with a Bonferroni correction. To visualize significant effects, we then ran a principal component analysis of the data using the base R function prcomp and visualized the results using the R package factorextra with the fviz_pca_biplot function (Kassambara & Mundt, 2020). Principal component scores for the first and second components were then extracted and statistically analyzed for: 1) correlation with immunological metrics (pearson correlation) and 2) association with factors of interest from the PERMANOVA (3-way repeated measures ANOVA; rstatix; (Kassambara, 2023). Representative scatter and box plots were constructed using ggplot2 (Wickham, 2016).

Following multivariate analyses, we examined each immune metric independently with univariate approaches, specifically a 3-way repeated measures ANOVA in the rstatix package. We incorporated fixed factors of interest: temperature, nutrients, immune challenge, and accounted for repeated sampling at the level of host genotype. Data was checked against appropriate statistical assumptions (normality, no outliers, etc.) prior to analyses and transformed when necessary. Posthoc analyses were conducted using pairwise T-tests with Bonferroni corrections. Representative box plots were constructed using ggplot2 (Wickham, 2016).

3.2. Results

3.2.1. Multivariate Analyses

PERMANOVA analysis revealed strong impacts of temperature, nutrients, and their interaction on combined immune metric data, but no impact of immune challenge (Table 7). Only 33% of the variance was explained by a factor or interaction of interest (residual $R^2 = 0.77$). Temperature accounted for nearly 10% of the variance in immune metrics ($R^2 = 0.0957$, p = 0.001), whereas nutrients accounted for only about 5% of the variance ($R^2 = 0.0473$, p = 0.009). Finally, the combined impact of nutrients and temperature accounted for an additional 3.6% of the variance ($R^2 = 0.0365$, p = 0.036). Pairwise analyses indicated significant differences between the high and mid nutrient groups only (padj = 0.021). Additionally, the Ambient+Mid treatment group was significantly different from all Heat treatment groups regardless of nutrient treatment (Table 8). Furthermore, Heat+Mid was significantly different from Ambient+None, and Heat+High (Table 8).

Table 7. PERMANOVA results for combined immunological metrics. Df= degrees of freedom. R^2 value gives an estimate of the amount of variance explained by a given factor. Bold font indicates significant p values (i.e. Pr(>F)).

Factor	Df	Sum of	\mathbb{R}^2	F	Pr(>F)
		Squares			
Temperature	1	31.8	0.0957	8.94	0.001***
Nutrients	2	15.7	0.0473	2.17	0.010**

18

Infection	1	3.10	0.00943	0.873	0.377
Temp*Nutrients		12.11	0.0365	1.70	0.045*
Temp*Infection	1	1.71	0.00515	0.482	0.653
Nutrients*Immune Challenge	2	10.56	0.0315	1.47	0.090
Temp*Nutrients*Immune	2	1.41	0.00424	0.198	0.979
Challenge					
Residual	72	256	0.770		
Total	83	332	1.00		

Principal component analyses demonstrated clear clustering as a result of temperature and nutrients, and some differentiation as a result of their combination (Figure 4). Principal components 1 and 2 explained a combined 65.4% of the variance in the data, 39.3% and 26.2% respectively. PC1 explained significant variance as a result of temperature treatment (Table 9; Figure 5a), while PC2 explained significant variance as a result of nutrient treatment and the interaction of nutrient treatments and immune challenge (Table 10, Figure 5b). Post-hoc analysis revealed that PC2 significantly reduced in response to immune challenge only in the absence of nutrient enrichment (*padj*=0.009). PC1 was significantly associated with all four immune metrics: negatively with catalase and positively with peroxidase, total phenoloxidase, and antibacterial activity (Figure 6). PC2 was significantly positively associated with catalase and total phenoloxidase only (Figure 7).

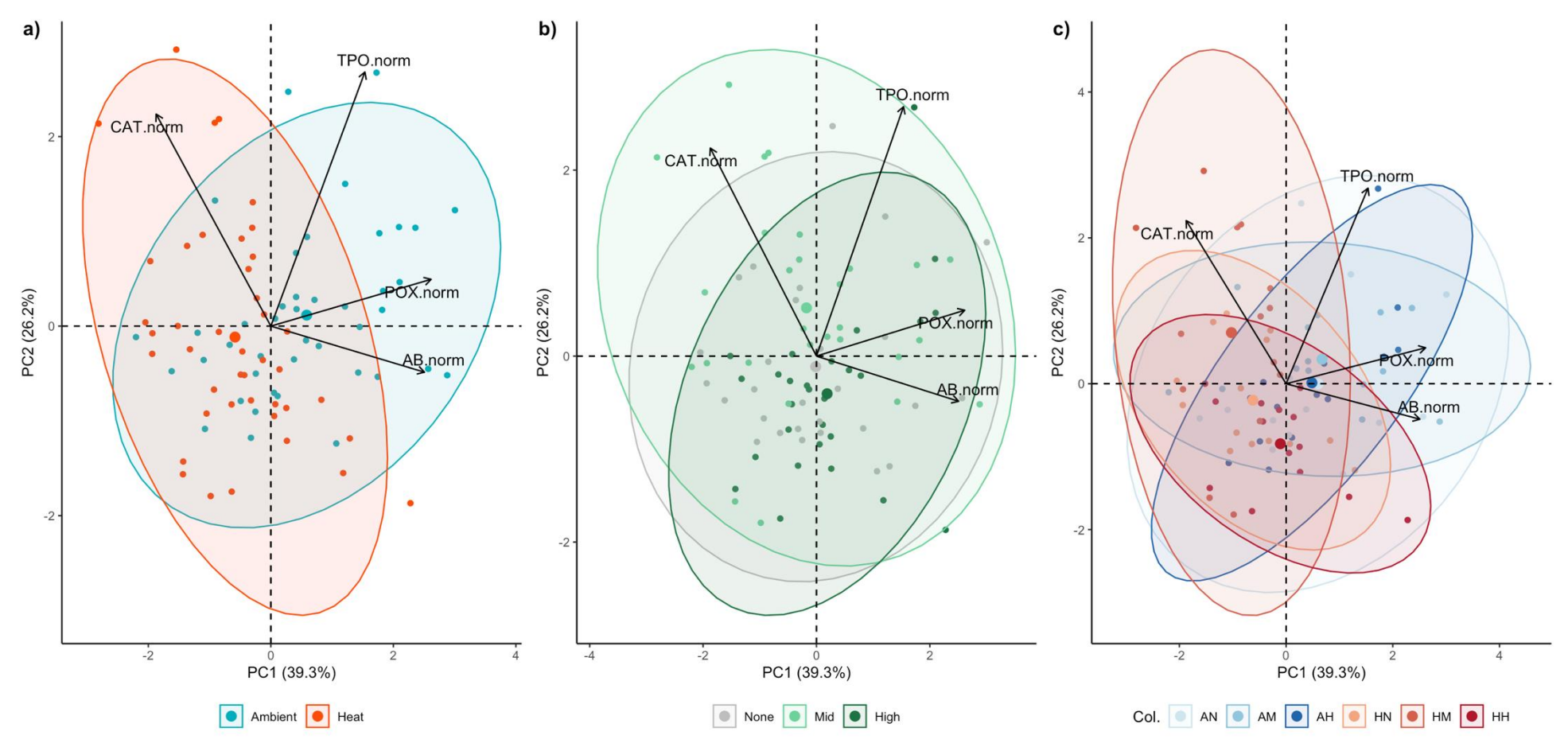


Figure 4. Biplot representation of PCA analysis of combined immune metric data. Plots are split based on groupings as follows: **a)** temperature treatment, **b)** nutrient treatment, **c)** temperature and nutrient combined grouping. In each case points represent individual sample points and are colored according to treatment group. Arrows eigenvector loadings of individual immune metrics, indicating direction in PC space and magnitude (i.e. length of line). Ellipses are drawn based on treatment groupings with 95% confidence intervals. PCA was visualized using the R package factoextra with the fviz pca biplot function.

Table 8. Pairwise PERMANOVA results for comparison of combined temperature and nutrient treatment groups. Reported are Bonferroni adjusted *p* values.

	Ambient, None	Ambient, Mid	Ambient, High	Heat, None	Heat, Mid
Ambient, Mid	1.0				
Ambient,	1.0	1.0			
High					
Heat, None	0.333	0.045*	0.36		
Heat, Mid	0.030*	0.030*	0.06	1.0	
Heat, High	1.0	0.045*	0.90	1.0	0.015*

Table 9. 3-way repeated measures ANOVA results investigating variance in PC1 as a result of temperature, nutrients, immune challenge and their interactions. Df= degrees of freedom. The ges value represents effect size of the factor of interest. Bold font indicates significant p values.

Effect	DFn	DFd	F	p	ges
Temperature	1	6	20.2	0.004*	0.232
				*	
Nutrients	2	12	0.825	0.462	0.019
Infection	1	6	0.161	0.702	0.001
Temp*Nutrients	2	12	2.96	0.090	0.043
Temp*Infection	1	6	0.170	0.694	0.0008
Nutrients*Immune Challenge	2	12	0.883	0.439	0.013
Temp*Nutrients*Immune	2	12	0.357	0.707	0.005
Challenge					

Table 10. 3-way repeated measures ANOVA results investigating variance in PC2 as a result of temperature, nutrients, immune challenge and their interactions. Df= degrees of freedom. The ges value represents effect size of the factor of interest. Bold font indicates significant p values.

21

Effect	DFn	DFd	F	p	ges
Temperature	1	6	1.07	0.341	0.017
Nutrients	2	12	6.29	0.014*	0.163
Infection	1	6	0.668	0.445	0.009
Temp*Nutrients	2	12	1.60	0.243	0.073
Temp*Infection	1	6	0.263	0.626	0.002
Nutrients*Immune Challenge	2	12	4.66	0.032*	0.063
				*	
Temp*Nutrients*Immune	2	12	0.406	0.675	0.005
Challenge					

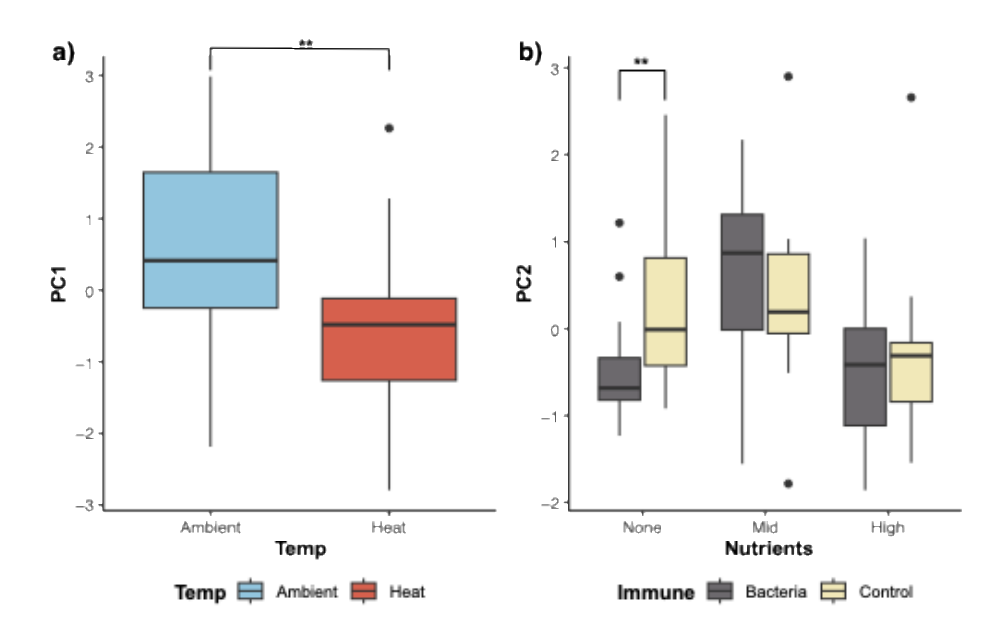


Figure 5. Box and whisker representing statistically significant variance of **a)** PC1 and **b)** PC2. Asterix indicates significantly different groups. Boxes are colored by treatment group (temperature or immune challenge).

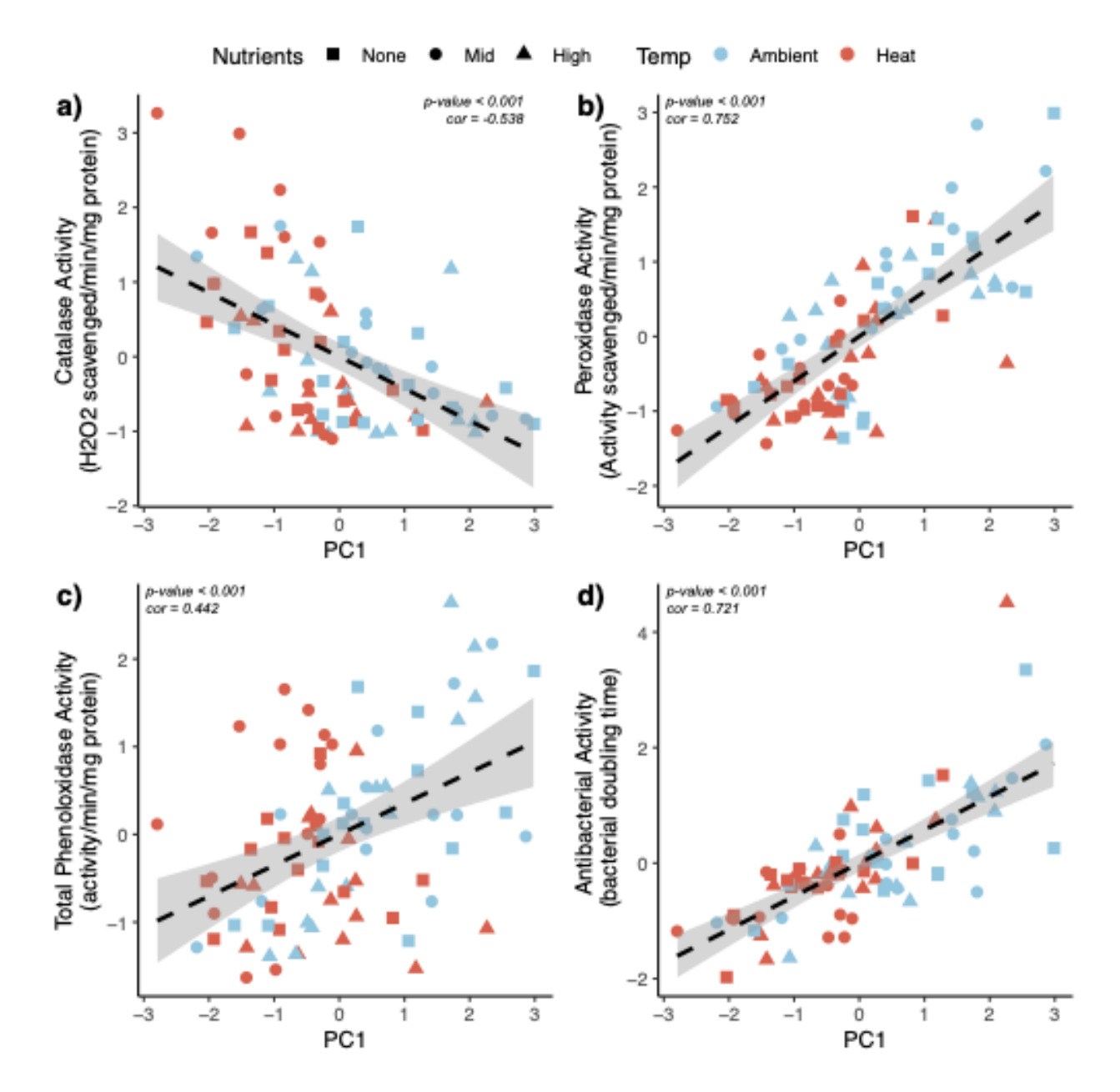


Figure 6. Correlation plot of the association of immune metrics with PC1 values: **a)** catalase activity, **b)** peroxidase activity, **c)** total phenoloxidase activity, **d)** antibacterial activity. For all graphs the normalized values used for PERMANOVA and principal component analyses are plotted. Points represent individual datum colored by temperature treatment and shaped by nutrients. Linear regression and 95% confidence intervals are plotted for each.

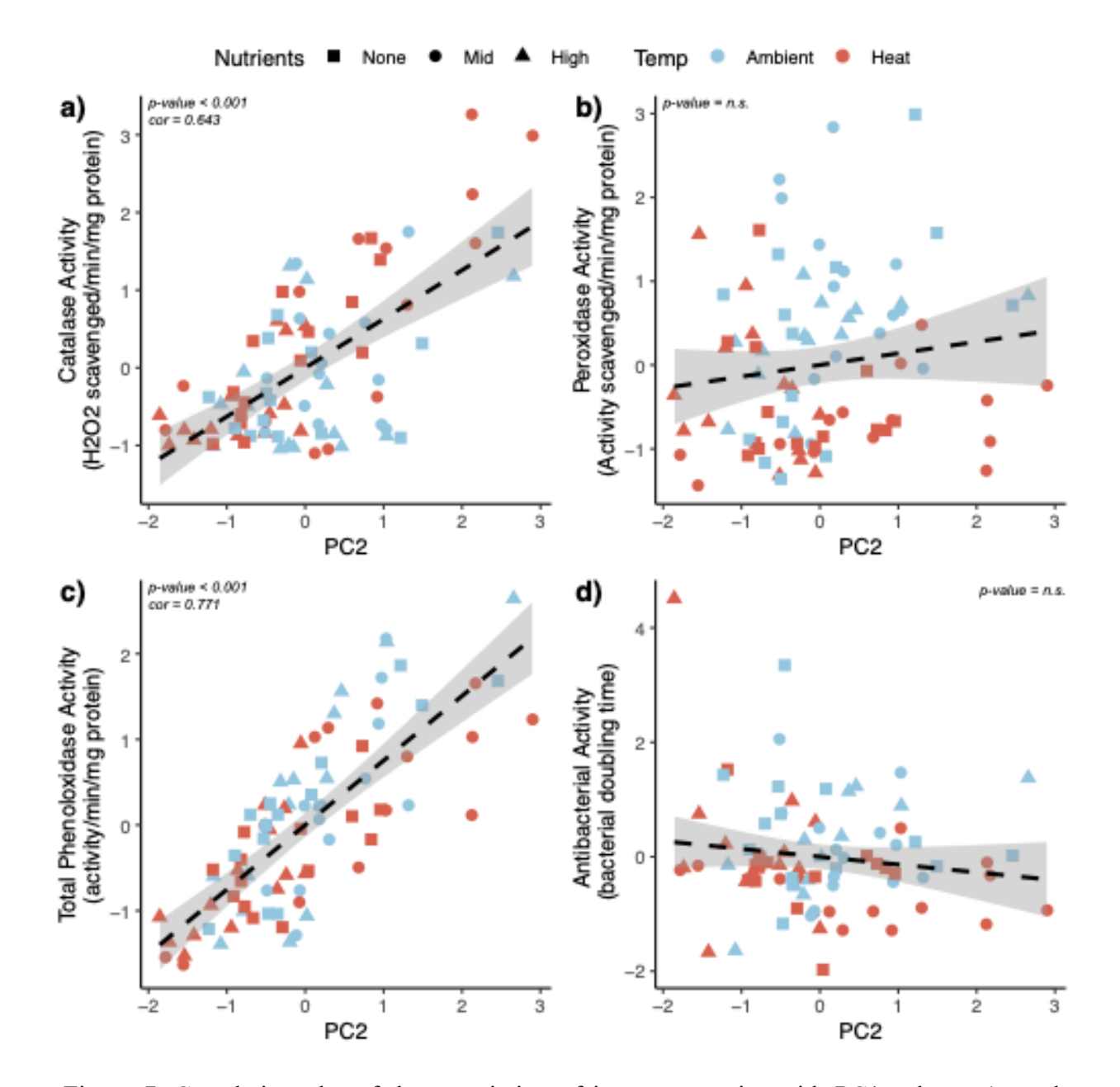


Figure 7. Correlation plot of the association of immune metrics with PC1 values: **a)** catalase activity, **b)** peroxidase activity, **c)** total phenoloxidase activity, **d)** antibacterial activity. For all graphs the normalized values used for PERMANOVA and principal component analyses are plotted. Points represent individual datum colored by temperature treatment and shaped by nutrients. Linear regression and 95% confidence intervals are plotted for each.

3.2.2. Univariate Analyses

Univariate analysis of individual immune metrics again revealed strong effects of both temperature and nutrient treatment, and some response to immune challenge. All immune metrics except for

24

catalase were significantly suppressed as a result of temperature treatment (Table 11, Figure 8b-d); catalase varied significantly as a result of nutrient treatment and the interaction of nutrients and immune challenge (Table 11, Figure 8a). Corals receiving mid nutrient treatments had significantly higher catalase activity after immune challenge than those high conditions regardless of immune challenge (Table 12, Figure 8a).

Table 11. 3-way repeated measures ANOVA results investigating variance in each immune metric individually as a result of temperature, nutrients, immune challenge and their interactions. Df= degrees of freedom. The ges value represents effect size of the factor of interest. Bold font indicates significant p values.

Catalase								
Effect	DFn	DFd	F	p value	ges			
Temperature	1	6	0.780	0.411	0.010			
Nutrients	2	12	9.165	0.004**	0.109			
					0.0006			
Infection	1	6	0.062	0.811	4			
Temperature:Nutrients	2	12	0.122	0.886	0.0030			
Temperature:Infection	1	6	1.559	0.258	0.016			
Nutrients:Infection	2	12	6.251	0.014*	0.113			
Temperature:Nutrients:Infecti								
on	2	12	2.316	0.141	0.045			
Peroxidase								
Effect	DFn	DFd	F	p value	ges			
				p<0.001*				
Temperature	1	6	46.5	*	0.262			
Nutrients	2	12	0.524	0.605	0.011			
Infection	1	6	2.13	0.195	0.015			
Temperature:Nutrients	2	12	1.60	0.243	0.055			
					0.0005			
Temperature:Infection	1	6	0.060	0.815	7			
Nutrients:Infection	2	12	01.09	0.368	0.013			
Temperature:Nutrients:Infecti								
on	2	12	0.538	0.598	0.011			
Total Phenoloxidase	Total Phenoloxidase							
Effect	DFn	DFd	F	p value	ges			
Temperature	1	6	5.67	0.055	0.053			
Nutrients	2	12	2.20	0.154	0.044			
Infection	1	6	0.528	0.495	0.005			
Temperature:Nutrients	2	12	0.406	0.675	0.020			
					0.0007			
Temperature:Infection	1	6	0.266	0.625	2			
Nutrients:Infection	2	12	2.21	0.152	0.021			

25

Temperature:Nutrients:Infecti						
on	2	12	0.187	0.717	0.003	
Antibacterial Activity						
Effect	DFn	DFd	F	p value	ges	
Temperature	1	6	8.29	0.035	0.100	
Nutrients	2	12	0.648	0.544	0.017	
Infection	1	6	2.286	0.191	0.077	
Temperature:Nutrients	2	12	1.20	0.341	0.027	
Temperature:Infection	1	6	1.08	0.346	0.004	
Nutrients:Infection	2	12	0.186	0.833	0.003	
Temperature:Nutrients:Infecti						
on	2	12	0.370	0.700	0.007	

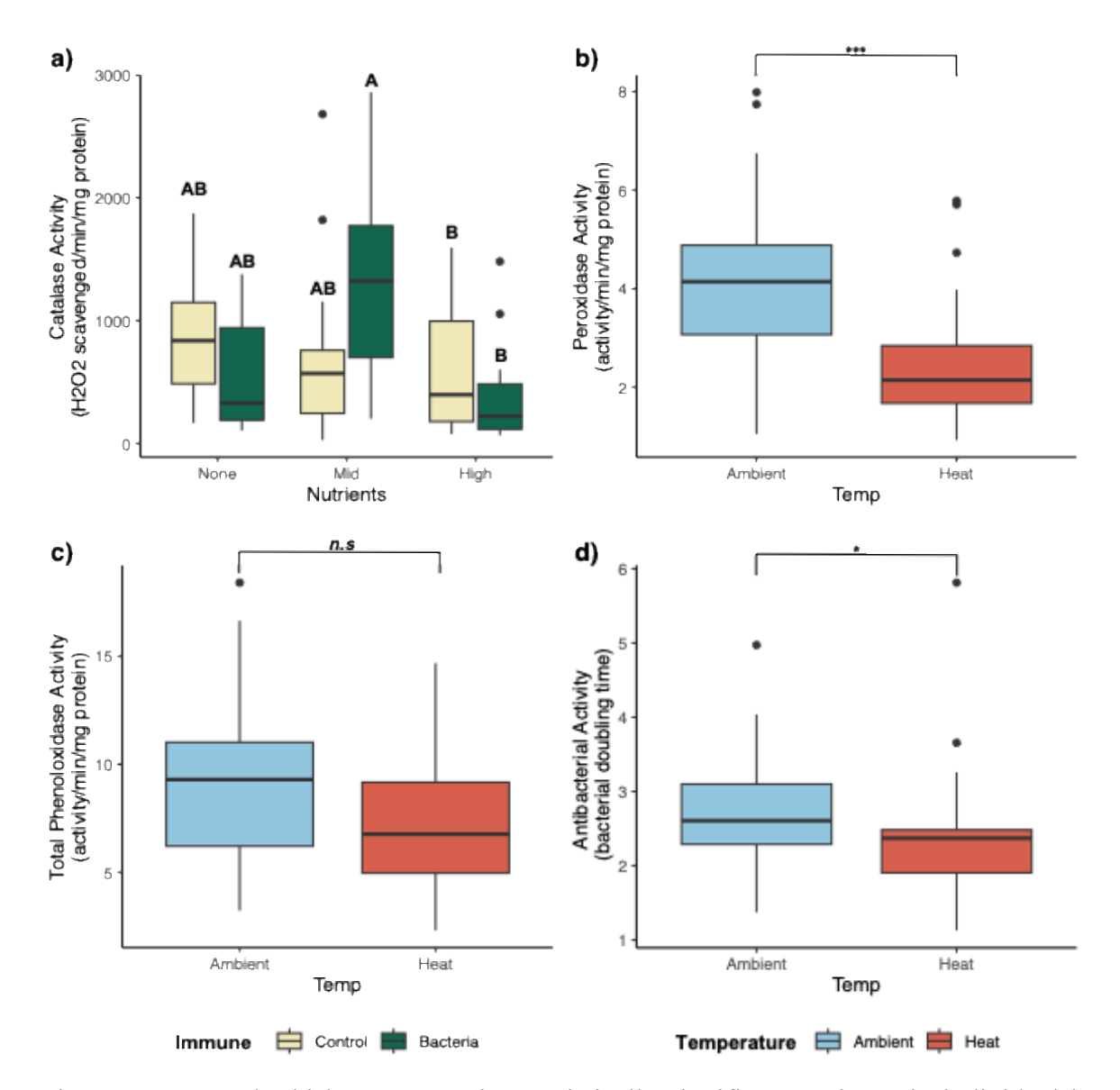


Figure 8. Box and whisker representing statistically significant variance in individual immune metrices **a**) catalase activity, **b**) peroxidase activity, **c**) total phenol oxidase activity, **d**) antibacterial activity. Letters indicate significant groups determined by post-hoc pairwise t-tests. Asterix indicates significantly different groups as indicated by the full 3-way repeated measures ANOVA model. Boxes are colored by treatment group (temperature or immune challenge).

Table 12. Results of post-hoc pairwise t-tests comparing groups of interactions between nutrient enrichment and immune challenge. Bold font indicates significant p values.

Comparison	stat	df	p	padj
High-Bacteria vs. High Control	-1.85	13	0.087	0.78
High-Bacteria vs. Mid-Bacteria	-6.37	13	< 0.001	<0.001***
High-Bacteria vs. Mid-Control	-1.33	13	0.208	0.98
High-Bacteria vs. None-Bacteria	-1.60	13	0.135	0.861
High-Bacteria vs. None-Control	-3.32	13	0.006	0.073
High-Control vs. Mid-Bacteria	-4.15	13	0.001	0.016*
High-Control vs. Mid-Control	-0.412	13	0.687	1.0
High-Control vs. None-Bacterial	-0.119	13	0.907	1.0
High-Control vs. None-Control	-1.92	13	0.077	0.769
Mid-Bacteria vs. Mid-Control	2.09	13	0.057	0.63
Mid-Bacteria vs. None-Bacteria	3.01	13	0.01	0.12
Mid-Bacteria vs. None-Control	1.65	13	0.123	0.861
Mid-Control vs. None-Bacteria	0.269	13	0.792	1.0
Mid-Control vs. None-Control	-1.36	13	0.196	0.98
None-Bacteria vs. Non-Control	-1.81	13	0.093	0.78

4. Goal 3: Model disease probability and identify resistant locations

4.1.Methods

The environmental parameters identified as significantly affecting disease susceptibility in goal 1 were recalculated with the most recent available environmental data to predict spatial variation in disease susceptibility across FCR. Monthly chlorophyll-a concentrations and PAR were extracted from NASA's Modis agua satellite from 2021 to 2024. The maximum chlorophyll-a concentration and maximum PAR were calculated as the mean of the maximum annual values at each satellite location. The three-month mean PAR was calculated as the mean annual PAR value at each satellite location. Maximum and three-month mean temperatures were calculated using in situ data from 2021 to 2022 at CREMP/SECREMP sites as in goal 1, as data was only available in the Florida Keys until mid-2023. The maximum temperature was calculated as the mean of the annual maximum at each site and the three-month mean as the mean temperature in the summer months (July, August and September). The environmental regime was then calculated at each DRM site surveyed throughout FCR in 2023 (n = 423) using a spatial join between the closest one to three satellite or CREMP/SECREMP sites, depending on distance between sites, as in goal 1. This current environmental regime was used in the fitted disease susceptibility GLMM, with M. cavernosa abundance at the DRM site used as the weights. No random effect structure was incorporated to give equal chance of disease prevalence across FCR. Inverse distance weighted interpolation was used to model disease probability across Florida in QGIS at 0.05° resolution with a distance coefficient, which controls the spatial rate of decay, of 10.

The environmental variables used in goal 2, ammonia and temperature, were also mapped across FCR. Mean annual maximum ammonia concentration was calculated using data collected as part of the Southeast Florida Reef Tract Water Quality Assessment Project and in the Florida Keys by the Southeast Environmental Research Center, where measurements encompass NH₃ and free NH₄⁺ ions. In the Coral AP, maximum ammonia concentration was calculated as the mean of the annual maximum from 2021 to 2024 from bottom samples collected at reef sites. In the Florida Keys, maximum ammonia was calculated as the mean of the annual maximum from 2021 to 2022. Maximum temperature was calculated as above at each CREMP/SECREMP site. Maximum ammonia concentrations and temperatures were interpolated across Florida with the same method as for disease probability.

4.2. Results

Predicted disease probability varied widely across FCR (Figure 8), but was generally higher in the Coral AP than the Florida Keys. The maximum disease probability was 0.31 offshore Port Everglades and was consistently above 0.1 (i.e., 10% of a disease outbreak) offshore northern Palm Beach and Martin counties. Disease probability was substantially lower (0.001) off the Broward-Miami border. In the Florida Keys, areas with low disease probability (< 0.01) were identified on the southern half of Key Largo and Tavernier in the upper keys, between northern Marathon and Layton in the middle keys, and offshore Lower Sugarloaf and Boca Chica Keys in the lower leys.

29 C40115

Increased disease probability (> 0.1) was predicted off northern Key Largo, off Lower Matecumbe Key and Long Key on the upper/middle keys border and in the channel off 7-mile bridge. Disease probability was substantially higher in the southwest of the Dry Tortugas National Park than in the northeast, although it did not exceed 0.1.

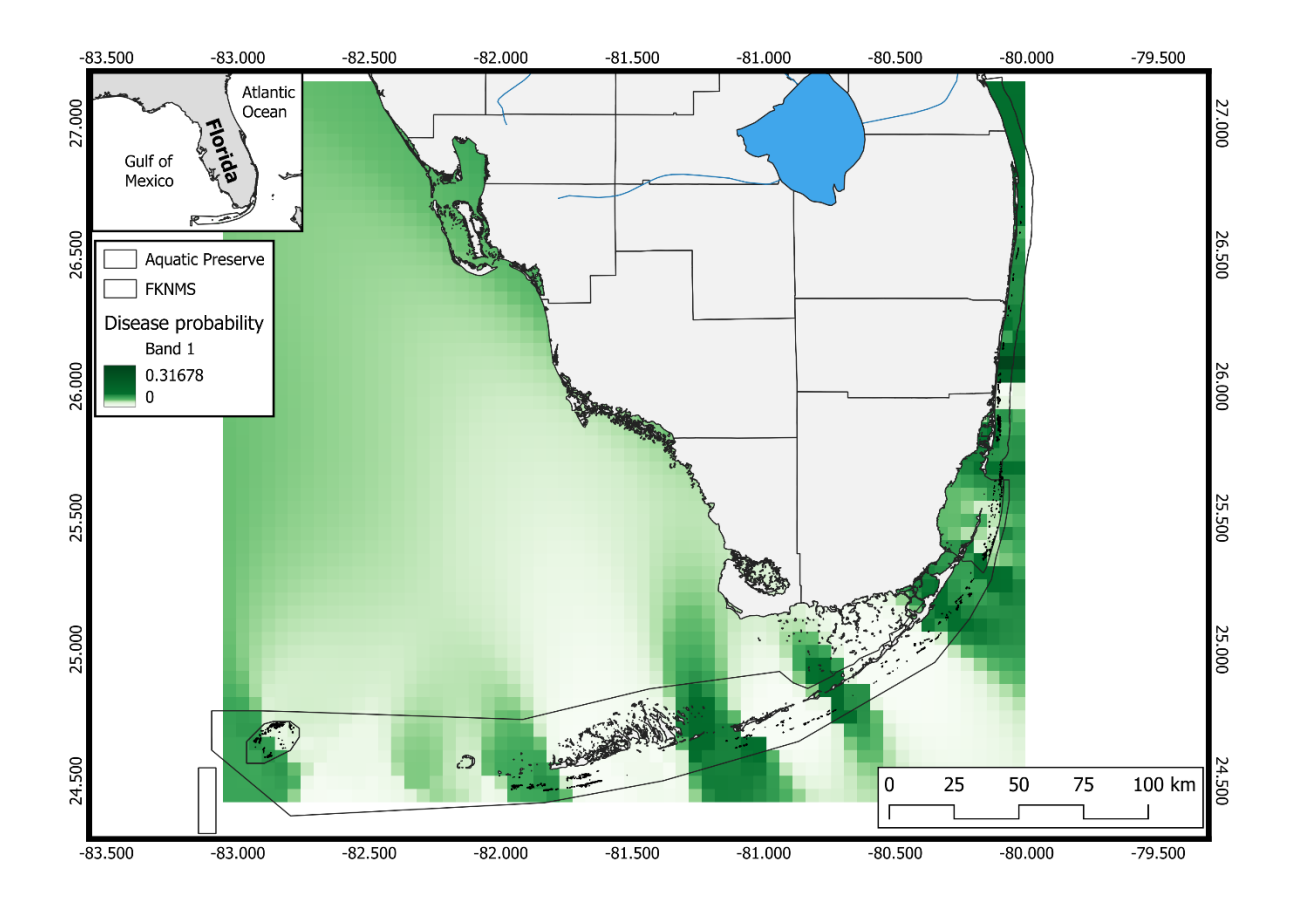


Figure 8. Predicted SCTLD probability calculated from refitted GLMM of disease susceptibility with current environmental regime at DRM sites and IDW interpolation across Florida at 0.05°. The darker the green, the greater the probability of disease, with a maximum disease probability of 0.31 offshore Port Everglades. Inset: Florida peninsula.

The mean maximum annual ammonia concentration was 0.016 mg/l across FCR and ranged two orders of magnitude from 0.06 mg/l off Boynton Beach to 0.0006 mg/l off Turtle reef in the upper keys. Ammonia concentration was consistently higher in the Coral AP than in the Florida Keys (Figure 9). Ammonia concentrations found to suppress immune response ($\geq 0.05 \text{ mg/l}$) were found at reef water quality monitoring sites near Jupiter, Boynton Beach and Boca inlets and near Government Cut.

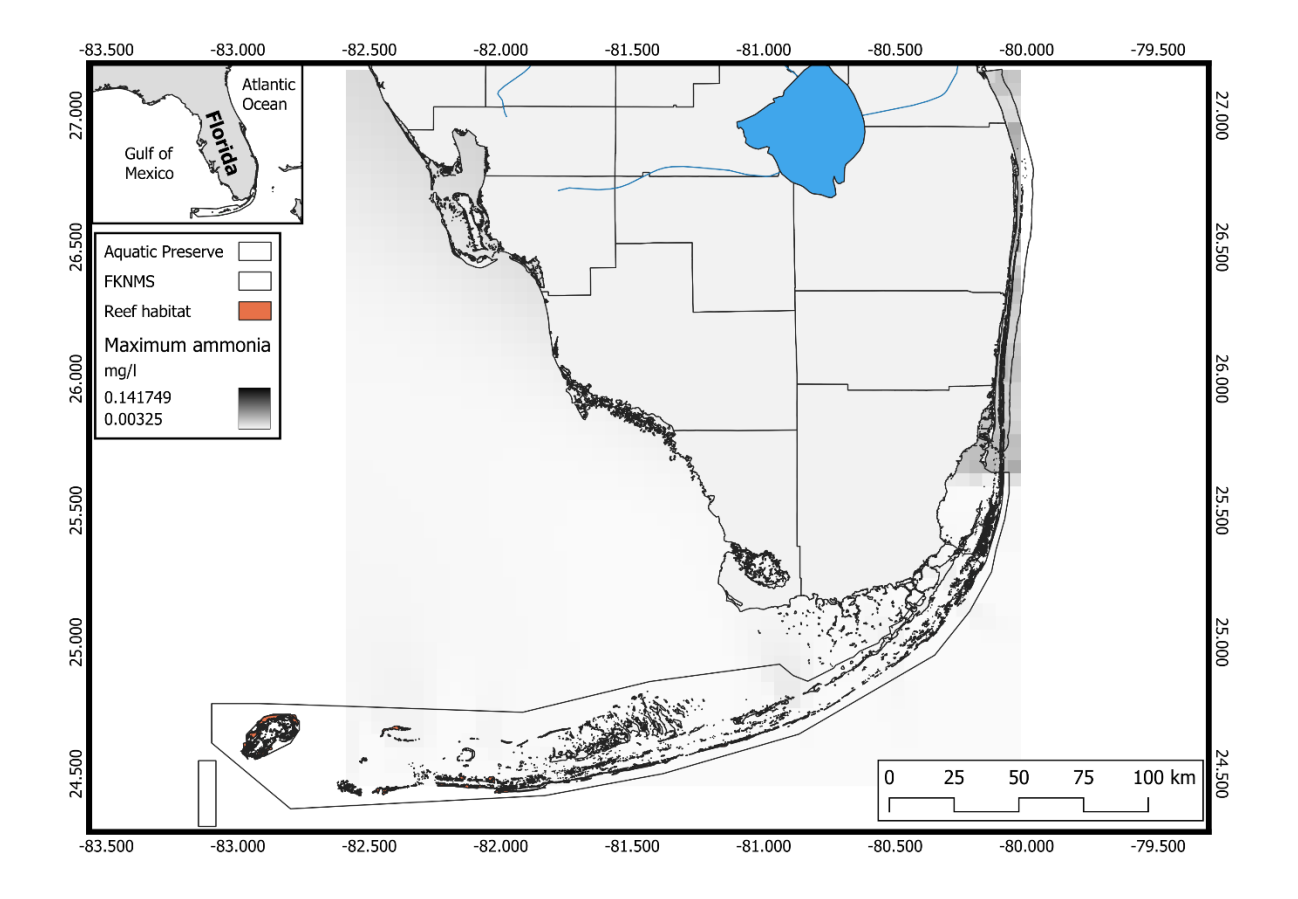


Figure 9. Maximum annual ammonia concentration across the FCR. Concentrations were measured from bottom samples as part of the Southeast Florida Reef Tract Water Quality Assessment Project in the Coral AP and in the Florida Keys by the Southeast Environmental Research Center. Inverse distance weighted interpolation was conducted to map ammonia concentrations across Florida at 0.05°. Inset: Florida peninsula. Note, in situ water quality data not available for the Dry Tortugas.

Mean annual ammonia concentrations across FCR were 0.006 mg/l and like maximum annual ammonia concentration, varied widely. Mean annual ammonia concentrations were nearly an order of magnitude higher in the Coral AP than in the Florida Keys, where they were below detectable limits in many locations. Conversely, at 40 of the 53 reef sites monitored within the Coral AP, mean ammonia concentrations were ≥ 0.01 mg/l in (Figure 10), the concentration found to elicit increased catalase activity when immune challenged.

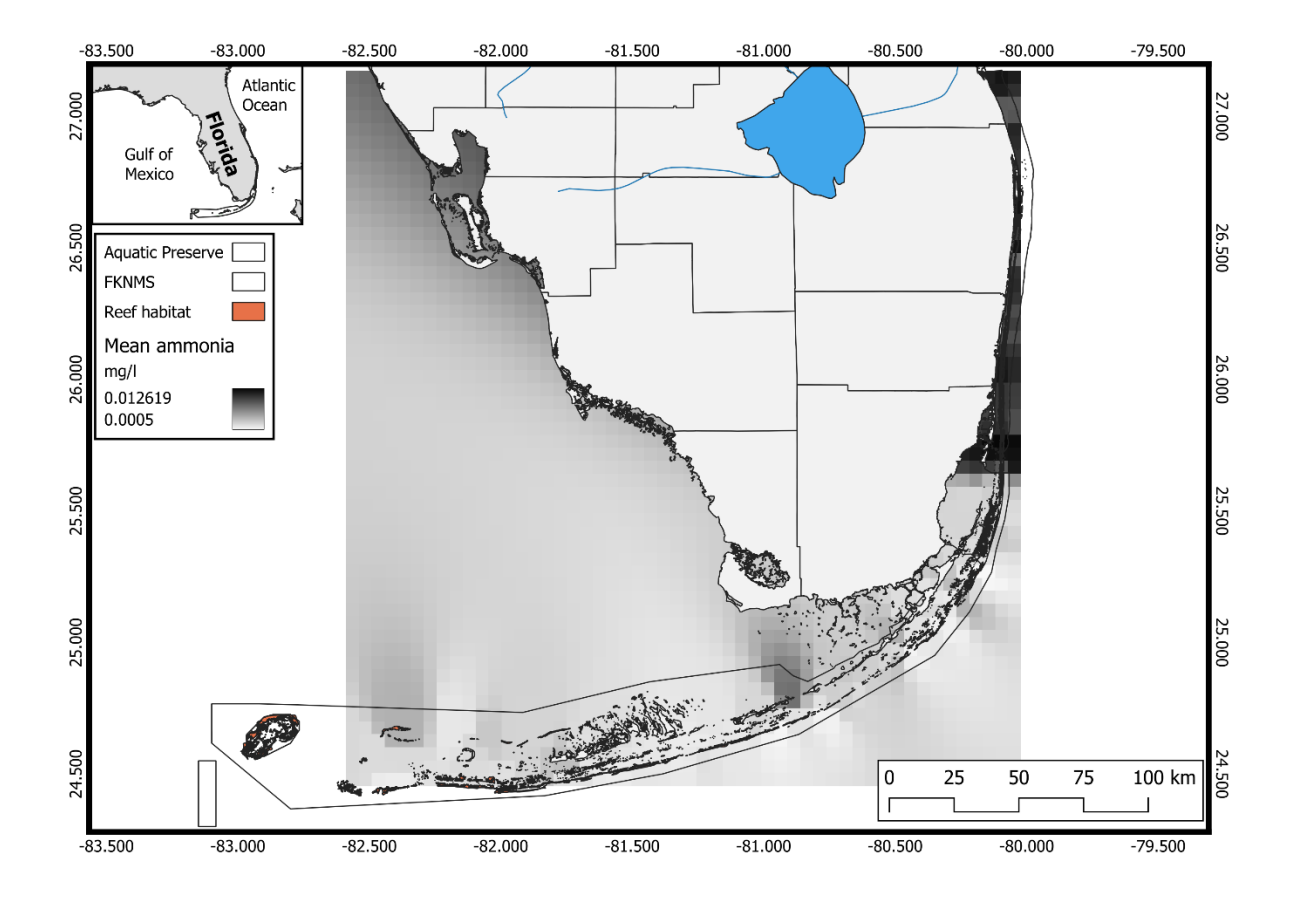


Figure 10. Mean annual ammonia concentration across the FCR. Concentrations were measured from bottom samples as part of the Southeast Florida Reef Tract Water Quality Assessment Project in the Coral AP and in the Florida Keys by the Southeast Environmental Research Center. Inverse distance weighted interpolation was conducted to map ammonia concentrations across Florida at 0.05°. Inset: Florida peninsula. Note, in situ water quality data not available for the Dry Tortugas.

In contrast to ammonia concentration, maximum temperatures were, unsurprisingly, higher throughout the Florida Keys than in the Coral AP. They were also noticeably cooler in the Dry Tortugas (Figure 11). The mean maximum annual temperature was 33.1 °C off Dove Key, a shallow hardbottom area off Key Largo. Exceptionally warm maximum temperatures (above 32.5 °C) were also measured at other shallow, inshore sites, El Radabob and Rattlesnake in the upper keys, Long Key and Moser Channel in the middle keys and Jaap Reef in the lower keys. Maximum temperatures at all sites exceeded 30.5 °C, the temperature frequently used as the coral bleaching threshold on FCR. Many SECREMP sites in the Coral AP and at Black Coral Rock, a deep pinnacle reef in the Dry Tortugas did not however, exceed 31 °C.

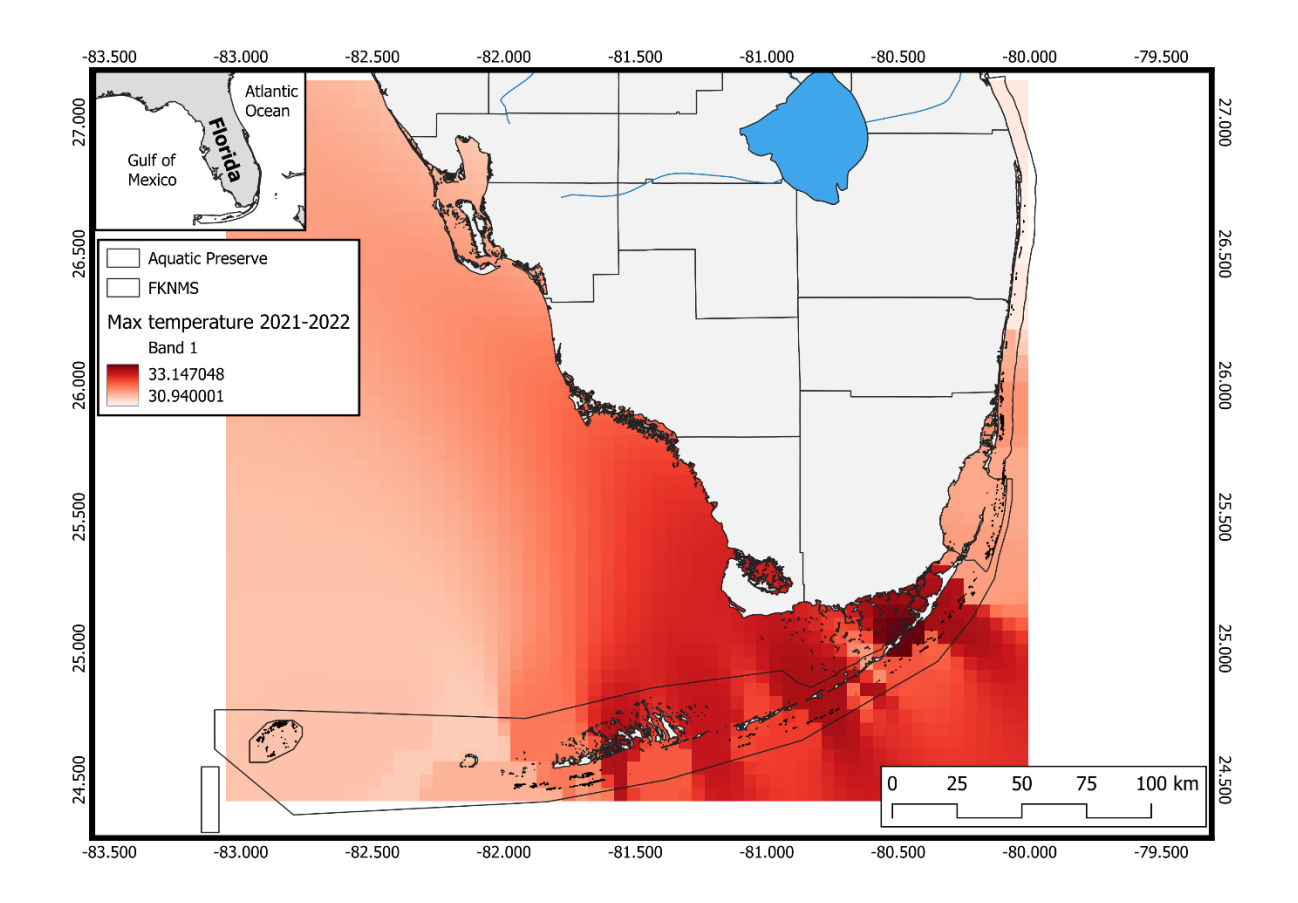


Figure 11. Mean maximum annual temperature from 2021 to 2022 measured from in situ loggers at CREMP/SECREMP sites throughout FCR. Inverse distance weighted interpolation was conducted to map maximum temperature across Florida at 0.05°. Inset: Florida peninsula.

5. Discussion and management recommendations

Statistical modelling found that environmental conditions significantly influenced Montastraea cavernosa's susceptibility to stony coral tissue loss disease and the severity of disease. Disease susceptibility was significantly influenced by temperature, light and chlorophyll-a concentration (nutrient proxy). Disease probability increased with the maximum temperature pre-survey when chlorophyll-a concentration was low, but was highest when chlorophyll-a concentration was high and the maximum temperature was lower (particularly below 28 °C). Disease susceptibility also increased with chlorophyll-a concentration when PAR was high, or when both chlorophyll-a and PAR were low, suggesting that the combined effect of high nutrients and light, or low nutrients and light increased disease susceptibility. Disease severity was only affected by the maximum temperature between surveys, with less than 50% chance a colony would die when temperatures exceeded the bleaching threshold. These findings support previous findings that suggest SCTLD initially affects Symbiodiniaceae before causing tissue loss in the coral host (Landsberg et al. 2020). While we used a proxy for nutrients (chlorophyll-a concentration), modelling results suggest disease susceptibility was highest under environmental conditions which would likely increase zooxanthellae production, i.e., high nutrients/chlorophyll-a and high light or high nutrients/chlorophyll-a and warm temperatures, but below the bleaching threshold. Further, that only maximum temperature affected disease severity suggests that once a colony becomes diseased, the probability of it surviving increased if temperatures exceeded the bleaching threshold.

Laboratory experimentation revealed significant effects of both temperature and nutrient stress, though no strong interactions between the two. Generally speaking, ecologically relevant high temperatures (32 °C) induced constitutive suppression of three prominent immunological metrics: peroxidase, antibacterial activity, and total phenoloxidase production. Furthermore, moderate levels of nutrients (0.01 mg/l ammonia) fundamentally changed the response of corals to pathogen stimuli. Under intermediate levels of nutrient enrichment, corals induced higher catalase activity in response to pathogen stimuli, whereas without nutrient enrichment (and marginally at high nutrient levels) levels of catalase and total phenoloxidase production decreased following pathogen stimulation. These preliminary results suggest optimal immune responses at moderate nutrient levels.

Our results suggest that temperature played the primary role in SCTLD susceptibility and severity and that it strongly influences immune response. Lab results found multiple immune metrics were suppressed at high temperatures, while enhanced catalase activity suggests stress within the coral host, suggesting further disease outbreaks are likely as ocean temperatures increase. While this appears to counter modelling results, it follows the same trend as the disease susceptibility model suggests under low nutrient/chlorophyll-a conditions. It is plausible that the difference is because SCTLD appears to affect the symbionts initially, but this is impossible to investigate without a known pathogen. Our results also suggest that generally under moderate ammonia concentration (0.01 mg/l) the coral host has enhanced immune response, until ammonia concentrations are very high (0.05 mg/l). Spatial analysis identified multiple locations that have enhanced and reduced disease susceptibility, which should be taken into account when choosing outplanting locations for

M. cavernosa. Spatial analysis also identified multiple locations, primarily near inlets in the Coral AP, where experimental nutrient enrichment conditions suggest immune response is suppressed. Reducing excess ammonia in these locations could therefore improve coral immunity and reduce the likelihood of another major disease outbreak.

6. References

Aeby GS, Ushijima B, Campbell JE, Jones S, Williams GJ, Meyer JL, Häse C, Paul VJ (2019) Pathogenesis of a tissue loss disease affecting multiple species of corals along the Florida Reef Tract. Frontiers in Marine Science 6:678.

Alvarez-Filip L, Estrada-Saldívar N, Pérez-Cervantes E, Molina-Hernández A, González-Barrios FJ. 2019. A rapid spread of the stony coral tissue loss disease outbreak in the Mexican Caribbean. PeerJ 7:e8069

Alvarez-Filip L, González-Barrios FJ, Pérez-Cervantes E, Molina-Hernández A, Estrada-Saldívar N (2022) Stony coral tissue loss disease decimated Caribbean coral populations and reshaped reef functionality. Communications Biology, 5(1), 440.

Ban SS, Graham NA, Connolly SR (2014) Evidence for multiple stressor interactions and effects on coral reefs. Global change biology, 20(3), 681-697.

Bruno JF, Selig ER, Casey KS, Page CA, Willis BL, Harvell CD, Sweatman H, Melendy AM (2007) Thermal stress and coral cover as drivers of coral disease outbreaks. PLoS biology, 5(6), p.e124.

Changsut I, Womack HR, Shickle A, Sharp KH, Fuess LE (2022) Variation in symbiont density is linked to changes in constitutive immunity in the facultatively symbiotic coral, Astrangia poculata. Biol Lett, 18(11), 20220273. https://doi.org/10.1098/rsbl.2022.0273

Donovan MK, Burkepile DE, Kratochwill C, Shlesinger T, Sully S, Oliver TA, Hodgson G, Freiwald J, van Woesik R (2021) Local conditions magnify coral loss after marine heatwaves. Science 372(6545):977-80.

Fuess LE, Pinzon C, JH, Weil E, Mydlarz LD (2016) Associations between transcriptional changes and protein phenotypes provide insights into immune regulation in corals. Dev Comp Immunol, 62, 17-28. https://doi.org/10.1016/j.dci.2016.04.017

Hayes NK, Walton CJ, Gilliam DS (2022) Tissue loss disease outbreak significantly alters the Southeast Florida stony coral assemblage. Frontiers in Marine Science 9: 975894.

Hartig F (2017) DHARMa: residual diagnostics for hierarchical (multi-level/mixed) regression models R package

Jones NP, Figueiredo J, Gilliam DS (2020) Thermal stress-related spatiotemporal variations in high-latitude coral reef benthic communities. Coral Reefs 39:1661-1673. https://doi.org/10.1007/s00338-020-01994-8

Jones NP, Kabay L, Semon Lunz K, Gilliam DS (2021) Temperature stress and disease drives the extirpation of the threatened pillar coral, Dendrogyra cylindrus, in southeast Florida. Scientific reports 11:14113

Jones NP, Gilliam DS (2024) Temperature and local anthropogenic pressures limit stony coral assemblage viability in southeast Florida. Marine Pollution Bulletin 200:116098

Kassambara A (2023) rstatix: Pipe-Friendly Framework for Basic Statistical Tests. In (Version R package version 0.7.2) https://rpkgs.datanovia.com/rstatix/

Kassambara A, Mundt F (2020) Factoextra: Extract and Visualize the Results of Multivariate Data Analyses. In https://CRAN.R-project.org/package=factoextra

Lapointe BE, Brewton RA, Herren LW, Porter JW, Hu C (2019) Nitrogen enrichment, altered stoichiometry, and coral reef decline at Looe Key, Florida Keys, USA: a 3-decade study. Mar Biol 166:108

Lesser MP, Bythell JC, Gates RD, Johnstone RW, Hoegh-Guldberg O (2007) Are infectious diseases really killing corals? Alternative interpretations of the experimental and ecological data. Journal of experimental marine biology and ecology, 346(1-2), 36-44.

Martinez Arbizu P (2020) pairwiseAdonis: Pairwise multilevel comparison using adonis. In (Version R package version 0.4)

Miller J, Muller E, Rogers C, Waara R, Atkinson A, Whelan KRT, Patterson M, Witcher B (2009) Coral disease following massive bleaching in 2005 causes 60% decline in coral cover on reefs in the US Virgin Islands. Coral Reefs, 28, pp.925-937.

Morris LA, Voolstra CR, Quigley KM, Bourne DG, Bay LK (2019) Nutrient availability and metabolism affect the stability of coral–Symbiodiniaceae symbioses. Trends in microbiology, 27(8), 678-689.

Muller EM, Van Woesik R (2009) Shading reduces coral-disease progression. Coral reefs, 28, 757-760.

Muller EM, Sartor C, Alcaraz NI, Van Woesik R (2020) Spatial epidemiology of the stony-coral-tissue-loss disease in Florida. Frontiers in Marine Science 7:163

Mydlarz LD, Palmer CV (2011) The presence of multiple phenoloxidases in Caribbean reefbuilding corals. Comp Biochem Physiol A Mol Integr Physiol, 159(4), 372-378. https://doi.org/10.1016/j.cbpa.2011.03.029

NOAA Coral Reef Watch. 2019, updated daily. NOAA Coral Reef Watch Version 3.1 Daily 5km Satellite Regional Virtual Station Time Series Data for Southeast Florida, Mar. 12, 2013-Mar. 11,

2014. College Park, Maryland, USA: NOAA Coral Reef Watch. Data set accessed 2020-02-05 at https://coralreefwatch.noaa.gov/product/vs/data.php

Oksanen J, Simpson G, Blanchet F, Kindt R, Legendre P, Minchin P, O'Hara R, Solymos P, Stevens M, Szoecs E, Wagner H, Barbour M, Bedward M, Bolker B, Borcard D, Borman T, Carvalho G, Chirico M, De Caceres M,... Weedon J (2025). vegan: Community Ecology Package. In (Version R package version 2.8-0) https://vegandevs.github.io/vegan/

Pollock FJ, Lamb JB, Field SN, Heron SF, Schaffelke B, Shedrawi G, Bourne DG, Willis BL (2014) Sediment and turbidity associated with offshore dredging increase coral disease prevalence on nearby reefs. PLOS One 9: e102498

Precht WF, Gintert BE, Robbart ML, Fura R, Van Woesik R (2016) Unprecedented disease-related coral mortality in Southeastern Florida. Scientific reports 6(1):31374

R Core Team (2024). R: A Language and Environment for Statistical Computing. R Foundation for Statistical Computing, Vienna, Austria. https://www.R-project.org/.

Rippe JP, Baumann JH, De Leener DN, Aichelman HE, Friedlander EB, Davies SW, Castillo KD (2018) Corals sustain growth but not skeletal density across the Florida Keys Reef Tract despite ongoing warming. Global Change Biology 24: 5205-5217

Shilling EN, Combs IR, Voss JD (2021) Assessing the effectiveness of two intervention methods for stony coral tissue loss disease on *Montastraea cavernosa*. Scientific reports, 11(1), 8566.

Van Woesik R, Randall CJ (2017) Coral disease hotspots in the Caribbean. Ecosphere, 8(5), e01814.

Vega Thurber RL, Burkepile DE, Fuchs C, Shantz AA, McMinds R, Zaneveld JR (2014) Chronic nutrient enrichment increases prevalence and severity of coral disease and bleaching. Global Change Biology 20: 544-554

Voss JD, Richardson LL (2006) Nutrient enrichment enhances black band disease progression in corals. Coral Reefs, 25, 569-576.

Walton CJ, Hayes NK, Gilliam DS (2018) Impacts of a regional, multi-year, multi-species coral disease outbreak in Southeast Florida. Frontiers in Marine Science, 5, 323.

Wickham H (2016) ggplot2: Elegant Graphics for Data Analysis. Springer-Verlag.

Williams SD, Walter CS, Muller EM (2021) Fine scale temporal and spatial dynamics of the stony coral tissue loss disease outbreak within the lower Florida Keys. Frontiers in Marine Science 8:631776